ELSEVIER

Contents lists available at ScienceDirect

Chemical Geology

journal homepage: www.elsevier.com/locate/chemgeo





Clumped and oxygen isotope sclerochronology methods tested in the bivalve *Lucina pensylvanica*

Jade Z. Zhang*, Sierra V. Petersen

Department of Earth and Environmental Science, University of Michigan, Ann Arbor, MI, USA

ARTICLE INFO

Editor: Don Porcelli

Keywords: Isotope Geochemistry Bivalve Subannual Clumped Isotope High Resolution Clumped Isotope

ABSTRACT

Geochemical signatures preserved within the geologic record can be used to reconstruct past mean temperature and seasonality, but in order to accurately apply any geochemical proxy method in the past, a rigorous study of how the recorded proxy is related to temperature in the modern setting must be conducted. Here, we assess the ability of multiple isotope techniques to correctly record mean annual temperature and seasonality in the bivalve Lucina pensylvanica. We compare subannual-resolution δ^{18} O-based, seasonally-targeted and continuous highresolution (H.R.) clumped isotope (Δ_{47})-based thermometry methods, as well as multiple data treatment methods for each, to determine which approach best matches known modern temperatures (maximum and minimum absolute temperature and annual temperature range), with the goal of defining the ideal sampling scheme for use on fossil shells. In L. pensylvanica shells collected from 7 sites, we observe neither mean temperature nor seasonal biases. Mean annual temperature is best matched by averaging all seasonally-targeted Δ_{47} temperatures. Seasonality is best matched by averaging $\delta^{18}O_{carb}$ -based temperatures from all summers and all winters before taking the difference. Of two data treatment approaches applied to the continuous high-resolution Δ_{47} -based temperatures, "data optimization" is apparently better at resolving smaller seasonal temperature differences. In contrast, "data smoothing" produces a temperature record unbiased by prior assignment of seasonal extremes and has the simultaneous ability to detect subannual variability in $\delta^{18}O_{w}$. However, accurate application of H.R. Δ_{47} methods must balance sampling resolution and growth rate. If sampling resolution is high enough relative to the growth rate (\sim 1 pt./month or better), we recommend continuous high-resolution Δ_{47} thermometry with data smoothing. If this resolution cannot be achieved due to slow growth rates or insufficient shell size, we recommend pairing subannual $\delta^{18}O_{carb}$ -based and seasonally-targeted Δ_{47} -based temperature reconstruction to acquire seasonal range in temperature and absolute temperature extremes.

1. Introduction

Small changes in seasonal temperature extremes can affect multiple elements of the Earth's climate system. For example, warming winters have increasing Colorado's mountain pine beetle infestation (Negrón and Cain, 2019) and warming summers over the Greenland Ice Sheet have exceeded the melting point, triggering extensive surface melting (Nghiem et al., 2012). Determining how seasonality has changed in the past across different mean climate states can help predict which areas may be impacted by uneven seasonal warming in the future. Quantifying past changes in seasonality can also be used to validate climate model simulations at a finer scale (Tierney et al., 2020) and improve mean annual temperature reconstructions through identifying seasonal biases in time-averaged proxy records (Ivany, 2012). However, in most

paleoclimate studies, reconstructed temperatures are often limited to long-term annual means, and paleoseasonality is overlooked. This is especially true in deep time, due to a variety of obstacles with the resolution and preservation of different climate archives (Ivany and Judd, 2021).

A common approach to reconstructing seasonal climate cycles in the past is through high-resolution oxygen isotope analysis (δ^{18} O) of fast-accumulating biogenic archives such as corals, mollusk shells or sponges (Shackleton, 1973; Corrège, 2006; Rosenheim et al., 2004). The oxygen isotopic composition of carbonate materials like shells or coral skeletons is related to the temperature of formation, equivalent to ocean temperatures for marine organisms (Epstein et al., 1953). Given the correct balance of sampling resolution and growth rate, sclerochronology, or sequential sampling of a shell or coral along its growth axis, can

E-mail address: jadezz@umich.edu (J.Z. Zhang).

^{*} Corresponding author.

therefore reveal subannual changes in environmental/ocean temperature (Schöne et al., 2004; Wanamaker et al., 2009; Wanamaker et al., 2011; Trofimova et al., 2018). However, this method also requires knowledge of the oxygen isotopic composition of the surrounding fluid $(\delta^{18}O_w)$ to reconstruct absolute temperatures (Epstein et al., 1953).

In many studies, $\delta^{18}O_w$ is assumed to be seasonally constant, albeit unknown, thus allowing calculation of the seasonal range in temperature from the measured range in $\delta^{18}O$ without quantitative knowledge of $\delta^{18}O_w$. However, without knowledge of $\delta^{18}O_w$, absolute maximum and minimum temperatures cannot be determined. The lack of direct knowledge of both the mean value and seasonal variability of $\delta^{18}O_w$ in ancient waters has limited the accurate application of the oxygen isotope paleothermometer in the past, both for paleoseasonality and mean temperature reconstructions. Paired measurements of trace element ratios and $\delta^{18}O$ have attempted to separate the influence of changing temperature and $\delta^{18}O_w$, but appear to require species-specific trace element calibrations, limiting their applicability further back in time (Gillikin et al., 2005). More recently, carbonate clumped isotope thermometry has risen as a tool to reconstruct past temperatures in the absence of prior knowledge of $\delta^{18}O_w$ (Eiler, 2007).

Carbonate clumped isotope (Δ_{47}) paleothermometry is a thermodynamically-based isotope proxy that leverages the temperature dependence of the internal ordering of the heavy isotopes ^{13}C and ^{18}O within the carbonate mineral lattice, specifically the abundance of carbonate ions containing both of these heavy isotopes bonded together (Ghosh et al., 2006; Eiler, 2011). This method enables direct estimation of the formation temperature of a carbonate material, independent of the surrounding water composition and is applicable to all types of carbonate materials, with no species-specific calibrations known to be needed for bivalves (Eiler, 2011; Henkes et al., 2013; Eagle et al., 2013; Wacker et al., 2014; Huyghe et al., 2022). When combined with traditional carbonate $\delta^{18}\text{O}$ paleothermometry, this technique also allows the simultaneous reconstruction of $\delta^{18}\text{O}_{w}$, providing valuable information about the formation environment (Eiler, 2007).

Until recently, large sample size requirements have limited application of clumped isotope paleothermometry to paleoseasonality reconstruction. Early measurements required 8-16 mg of CaCO₃ powder per replicate for a total of 24–48 mg for the typical three replicates (Ghosh et al., 2006; Tripati et al., 2010). Subsequently, sample sizes for individual replicates decreased to 3-5 mg on most machines, still requiring 12-20 mg in total to achieve good precision (Defliese et al., 2015; Daëron et al., 2016; Kelson et al., 2017). Compared to the 20–200 µg typically needed for single δ^{18} O analyses, this larger sample size requirement for Δ_{47} and need for triple replication largely prohibited the acquisition of subannual and/or high-resolution Δ_{47} -based temperature records (Keating-Bitonti et al., 2011).

Engineer advances now allow clumped isotope analysis of much smaller amounts of material (~150-450 μg per replicate) on certain instrumental set ups (Kiel device, Schmid and Bernasconi, 2010; NuCarb device, Mackey et al., 2020), opening the possibility of subannual Δ_{47} records. In one approach (Δ_{47} sclerochronology), individual aliquots drilled sequentially along the direction of growth, as in typical δ^{18} Obased sclerochronology, are each analyzed once for Δ_{47} , then data from multiple adjacent aliquots is combined in different ways in postprocessing ("smoothing", "binning", or "optimization") to reduce uncertainty on calculated temperatures (de Winter et al., 2021; Caldarescu et al., 2021; Agterhuis et al., 2022). Another approach that addresses seasonal temperature fluctuations while working within sample material constraints (called seasonally-targeted Δ_{47}) combines highresolution δ^{18} O-based sclerochronology with a few, targeted bulk Δ_{47} analyses. In this method, summers and winters are assumed to correspond to δ^{18} O minima and maxima, respectively (Zhang et al., 2021). These intervals are then re-drilled to acquire one larger homogenized sample per seasonal extreme, which is replicated three times (Zhang et al., 2021). Assuming summers and winters are correctly identified, this method quantifies absolute temperature extremes and seasonal

 $\delta^{18}O_w$ variability but does not produce a continuous annual record of changing conditions. Depending on shell size, growth rate, sampling resolution, drill bit size, and geochemical reproducibility for a given instrument, one of these methods may be preferable over the other.

As these techniques are newly being applied at subannual scale, it is prudent to first validate these approaches using modern shells collected from sites where climate parameters (mean annual temperature, seasonality, $\delta^{18}O_{sw}$) are known. Validation in the modern can identify any biases in how these isotopic parameters are recorded in the shell or measured in the lab before the techniques are applied to fossil shells. For example, some calcifying organisms such as shallow water corals do not precipitate their skeletons in isotopic equilibrium with seawater, instead creating a calcifying fluid with a pH elevated relative to the surrounding seawater (Thiagarajan et al., 2011; Spooner et al., 2016), leading to offsets in Δ_{47} from values predicted for the known growth temperature. The presence of chemical symbionts in many species of the family Lucinidae (Taylor and Glover, 2000) raises the possibility of symbiont-induced vital effects, which could manifest as offsets in Δ_{47} , as seen in corals.

In this study, we aim to determine whether *Lucina pensylvanica*, and by extension related species of this genus, can correctly record mean annual temperature (MAT), maximum and minimum seasonal temperatures (Tmax and Tmin) and mean annual range in temperature ("seasonality" or MART). We compare results from $\delta^{18}\text{O}$ sclerochronology, seasonally-targeted Δ_{47} and Δ_{47} sclerochronology and assess how best to combine data from multiple years of shell growth to match modern climate most closely. We compare the performance of these different paleothermometry methods in areas with moderate (Florida) to more muted seasonality (Caribbean). Lastly, we discuss how to choose the most reliable sampling approach and data interpretation for paleotemperature and paleoseasonality reconstruction.

2. Materials and methods

2.1. Lucina pensylvanica

The bivalve Lucina pensylvanica belongs to the family Lucinidae. L. pensylvanica first appeared in the Pleistocene (Taylor and Glover, 2000; Yanes et al., 2012) and fossils in the family Lucinidae have been found dating back to the Silurian (Taylor and Glover, 2006). Species within this family are found today across a latitude range of 9° to 35°N, and members of the broader order Lucinida live over an even wider latitude range from 55°S to 60°N (Allen, 1958; Yanes et al., 2012). L. pensylvanica occupies predominantly shallow-water habitats, with substrates ranging from fine, intertidal muds to coarse sandy seagrass beds to organic rich sediments (Allen, 1958; Taylor and Glover, 2000; Yanes et al., 2012). In at least 30 species within Lucinidae (including L. pensylvanica), symbiotic sulfur-oxidizing bacteria have been detected in the gill filaments, acquired from and specialized for the specific surrounding environment (Taylor and Glover, 2000; Brissac et al., 2011). Shells of L. pensylvanica consist of three distinct aragonitic layers, identifiable in hand-sample and under scanning electron microscopy

Numerous studies on the feeding, respiratory systems, physiology, morphology, and mode of life of Lucinidae have been conducted (e.g., Allen, 1958; Taylor and Glover, 2000; Yanes et al., 2012). However, little attention has been paid to their potential as a recorder of past climate and seasonality. Previous studies of *L. pensylvanica* from the Florida Keys and Bahamas suggest that this species spawns in the warm season (Bigatti et al., 2004) and grows rapidly until sexual maturity is reached at a size of 25 mm in the Florida Keys (Taylor et al., 2004) or 18 mm in the Bahamas (Yanes et al., 2012), after which growth rates slow down. In the Florida Keys, shell size asymptotes around 38 mm at a maximum age of 5 years (Culotta, 1988; Bigatti et al., 2004; Taylor et al., 2004). Studies suggest that shell growth in *L. pensylvanica* occurs yearround, but growth rates may decrease during the warmest months due

to heat stress or reproduction (Bigatti et al., 2004; Yanes et al., 2012).

2.2. Study areas and modern climatology

Seven single valves of *L. pensylvanica* were collected from three beaches in Florida and four in the Caribbean. Florida sites include Cocoa Beach (CBFL; 28.3°N, 80.6°W); Hollywood Beach (HBFL; 26.0°N, 80.1°W); and Miami (25.7°N, 80.2°W). Caribbean sites include Montego Bay, Jamaica (18°N, 77°W); Cartagena, Colombia (10.3°N, 75.4°W); San Blas Island, Panama (9.5°N, 78.8°W); and St. Thomas, U.S. Virgin Island (18°N, 64°W) (Fig. 1). All shells were collected between 2018 and 2020. Although deceased, separated and lacking all fragile external lamellae due to wear (Taylor et al., 2004), collected valves show no signs of dissolution or more significant wear, so are assumed to have died within the past few years and thus record recent seawater temperatures in their shell geochemistry. Shell collection was completed by the crowdsource citizens science program, allowing us to easily sample from multiple sites, leveraging travel of others.

Modern seasonal patterns in temperature and precipitation were determined for each site from the NOAA NCDC ERSST v5 and CRU 3.25 Global Precipitation Data Set, respectively (https://iridl.ldeo.columbia.edu/SOURCES/.NOAA/.NCDC/.ERSST/.version5/.sst/), by averaging the past 60 years of data (1960–2022). Observed monthly mean sea surface temperatures (SSTs) from the Florida sites range from 21.6 to 23.5 °C in winter and up to 29–29.9 °C in summer, respectively (Fig. S1A, Table S2), with a seasonal range of 7.4 °C in more northerly CBFL and 6.4 °C in the more southerly HBFL and Miami. All three of these sites experience two-peak rainy seasons with highest rainfall occurring in June and August/September, although the peaks are quite muted in CBFL. Seasonal Variance in Precipitation (SVP), calculated as the difference between the rainiest and driest monthly precipitation means (Fig. S1B), ranges from 133 mm in CBFL to 183 in Miami to 196 mm in HBFL.

In contrast, seasonality at the Caribbean sites is much more muted, ranging from 26 to 27 $^{\circ}$ C in winter to 28.6–29.4 $^{\circ}$ C in summer (Fig. S1A, Table S2), for a total seasonal range of 1.8–2.9 $^{\circ}$ C. SVP in the Caribbean sites is greater compared to Florida sites, with the greatest SVP occurring in Panama (266 mm) due to high monthly rainfalls in May and October/November and in Colombia (219 mm) due to very dry months of

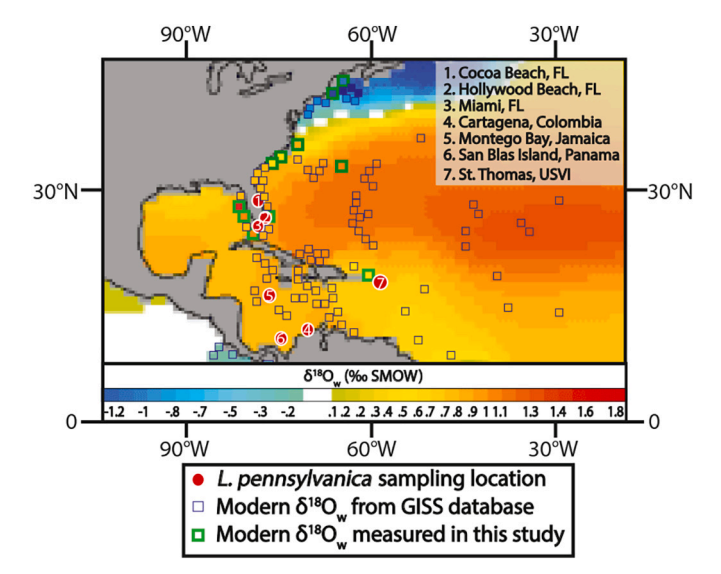


Fig. 1. Location of study sites, background plotted using modified LeGrande and Schmidt (2006) global gridded data model. Detailed information on measured modern $\delta^{18}O_w$ values can be found in supplement. Colour inside the $\delta^{18}O_w$ points are GISS/measured values overplotted onto the gridded model.

January/February (Fig. S1B). A two-peak rainy season is also experienced in all Caribbean sites, but the timing is different than in Florida, with the first peak occurring earlier (May) and the second peak occurring later (September/October/November) with moderately high rainfall in between (Fig. S1).

Mean annual temperature (MAT) was calculated as the mean of 12 monthly mean sea surface temperature. Mean annual range in temperature (MART) was calculated as the difference between the warmest and the coldest month. Season-to-season range in temperature (SRT) was calculated as the difference between the summertime (Jun-Jul-Aug) and wintertime (Dec-Jan-Feb) 3-month mean sea surface temperatures. SRT is always smaller than MART, and may be a better comparison point when growth rates are slower and seasonally-targeted sampling combines multiple warm/cold months into a single sample.

2.3. Physical parameters

Morphometric measurements were made on each shell, including 1) maximum valve length, from umbo to ventral margin; 2) maximum valve width, perpendicular to valve length, across the widest part of the shell; 3) valve weight (Fig. 2). These parameters were compared to each other and to mean annual temperature and shell age, as defined by stable isotope sclerochronology profiles (see below) (Fig. 3). One shell (CBFL) was imaged under scanning electron microscopy to confirm the assumption of minimal post-depositional alteration and visualize shell microstructures. Documenting the appearance of shell microstructures in modern, well-preserved shell valves is a valuable reference point for future studies on fossil shells, where preservation is uncertain.

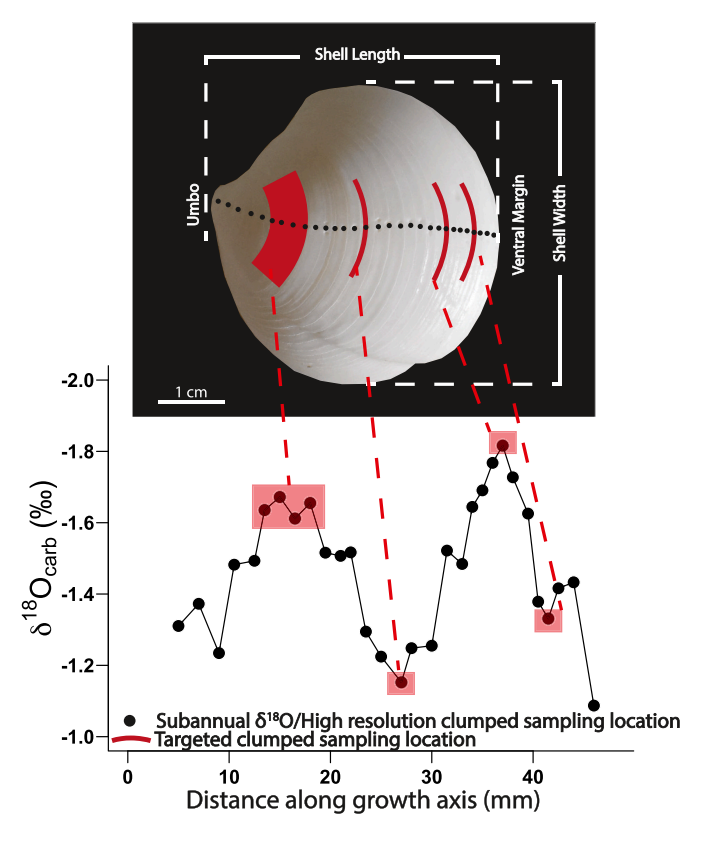


Fig. 2. Annotated image of modern *L. pensylvanica* shell (sample from Jamaica) showing high resolution δ^{18} O/ Δ_{47} drilling spots (black) and larger seasonally-targeted Δ_{47} sampling locations (red) as well as morphometric measurements. (For interpretation of the references to colour in this figure legend, the reader is referred to the web version of this article.)

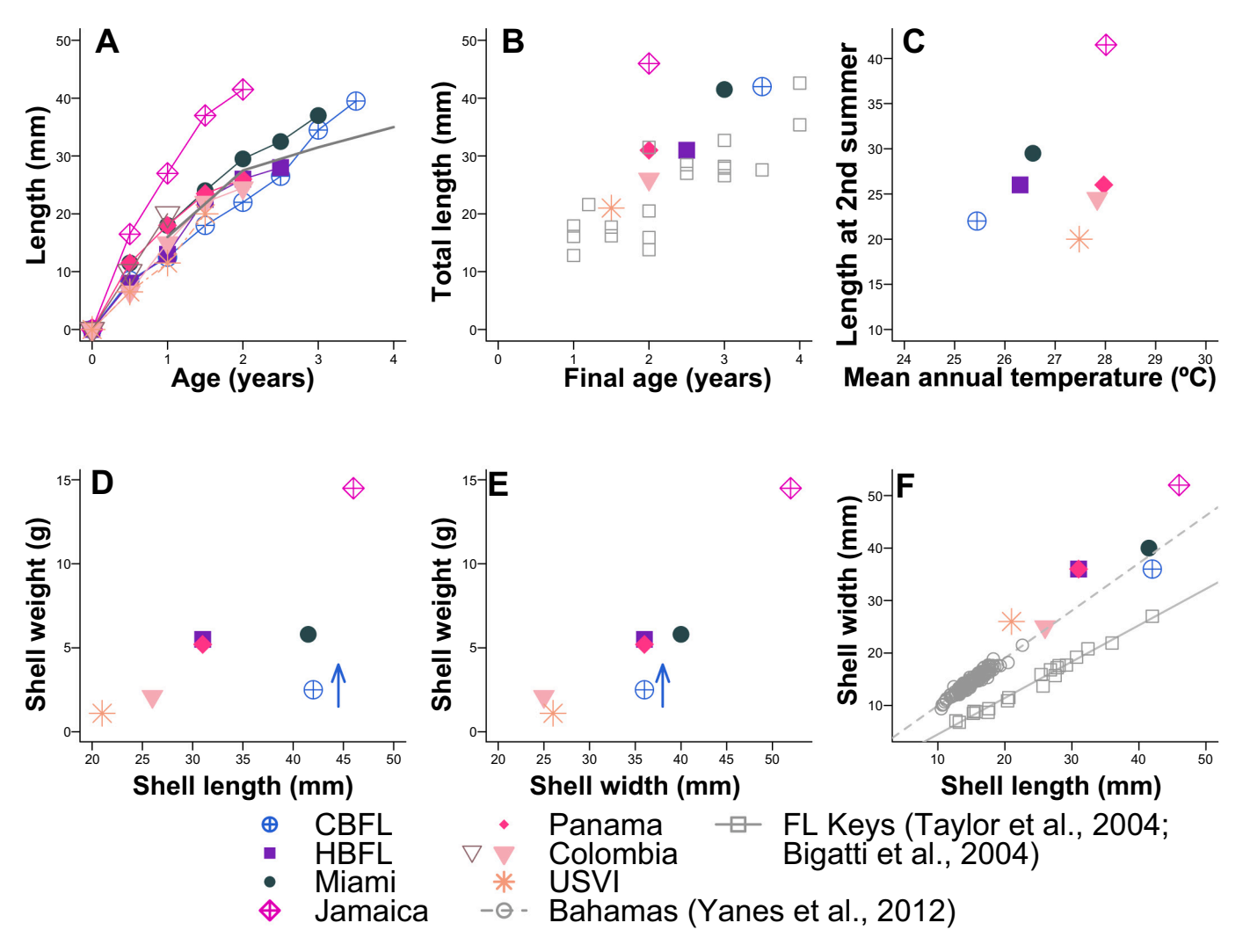


Fig. 3. Linear morphometric measurements of seven *L. pensylvanica* shells, and physical parameter data from two previous studies (Taylor et al., 2004; Bigatti et al., 2004; Yanes et al., 2012) are included here for comparison. Growth adjusted for the Colombia shell based on H.R. Clumped measurements (See discussion).

2.4. Sampling for isotopic analysis

All *L. pensylvanica* valves were sampled serially from umbo to ventral margin for $\delta^{18}O$ (and $\delta^{13}C$) sclerochronology. Drilling was conducted along the axis of maximum growth using a dental drill operated at its lowest speed (1000 RPM) to prevent frictional heating that can alter Δ_{47} (Fig. 2). A 0.8 mm scriber point carbide tip was used for $\delta^{18}O$ sampling; and a 1.4 mm inverted cone carbide tip was used for Δ_{47} sampling. Drill holes were kept shallow as to only penetrate the outer most shell layer (\sim 0.5 mm depth) to avoid crossing growth lines, and were spaced every \sim 1.5 mm, resulting in a resolution of 10–15 points per year of growth. Drilling began 8 mm from the umbo on the Miami shell due to the outer layer being broken off nearest the umbo. Similarly, the drill path deviated laterally from the axis of maximum growth on the CBFL shell due to roughly ½ of the shell being broken off near the ventral margin (Fig. S3).

Maxima and minima from each δ^{18} O profile were resampled using the same low speed dental drill to collect a total of ~20 mg of homogenized calcium carbonate powder per drill location for seasonally-targeted Δ_{47} analysis (Fig. 2). Drill zones were extended laterally from the midline (axis of maximum growth) to gather enough material while minimizing time averaging (Fig. 2). Final drill zone sizes ranged from 10 to 30 mm wide and 1 to 3 mm along the growth axis and were roughly 0.5 mm deep. Depending on the size of the shell and number of years of growth, 2 to 6 points were analyzed per shell for seasonally-targeted Δ_{47} .

Two *L. pensylvanica* specimens (Miami, Colombia) were chosen for high resolution (H.R.) Δ_{47} sclerochronology to test the ability to quantify seasonal variability in temperature and $\delta^{18}O_w$ in a lower- and higher-seasonality environment using continuous sampling approaches. New samples were drilled from umbo to ventral margin, following the same sampling path and resolution as for $\delta^{18}O$ sclerochronology (Fig. 2). For the Miami shell, approximately 3-4 mg of powder was collected at each point, enough for a single replicate in "bellows mode" (see below). In contrast, for the Colombia shell, aliquots of 350–450 µg were drilled at each position for analysis in "coldfinger mode" (see below).

2.5. Stable oxygen and carbon isotope analysis

Each carbonate powder was analyzed for $\delta^{13} C$ and $\delta^{18} O$ using a Kiel IV automated carbonate preparation device attached to a Thermo-Finnegan MAT 253 or Delta V dual inlet mass spectrometer at the University of Michigan Stable Isotope Lab. Data was standardized against NBS-18 and NBS-19 with units reported in per mille (‰), relative to the VPDB standard, with a typical uncertainty of $\pm 0.1\%$ or less in both $\delta^{13} C$ and $\delta^{18} O$.

Assuming a constant $\delta^{18}O_w$ value, each $\delta^{18}O_c$ value was converted to temperature using the water-aragonite fractionation factor of Kim et al. (2007). Temperatures were derived using two different $\delta^{18}O_w$ values: 1) instrumental $\delta^{18}O_w$ values taken from either the GISS $\delta^{18}O_w$ database or new measurement as part of this study (see below), or 2) shell mean

 $\delta^{18}O_{w}$ values calculated by averaging 2–6 seasonally-targeted Δ_{47} measurements (see below).

2.6. Clumped isotope analysis and data processing

Clumped isotope analyses were carried out on a Nu Instruments Perspective isotope ratio mass spectrometer connected to a NuCarb automated carbonate sample preparation device in the University of Michigan Stable Isotope SCIPP Lab in one of two different modes (O'hora et al., 2022; Jones et al., 2022). "Bellows mode" was used for all seasonally-targeted Δ_{47} and Δ_{47} sclerochronology on the Miami shell. "Coldfinger mode" was used for Δ_{47} sclerochronology on the Colombia shell. These two different modes were each used to be able to compare and test the accuracy and applicability of each analysis type.

In "bellows mode", approximately 3-4 mg of powder was loaded into an individual sample vial, placed in a carousel within the Nu Carb device (maintained at 70 °C). 150 µl of 105 wt% H₃PO₄ was injected into the sample vial and after being isolated for the first five minutes to prevent vigorous bubbling driving acid into the valves, the vial was opened to a liquid-nitrogen cooled trap where CO2 was collected for a further 15 min. Collected CO2 was separated from water via two variabletemperature traps and cleaned of contaminants by passing over silver wool and a cryo-cooled trap containing PorapaqQ material (-30 °C, 15 min). Lastly, purified CO2 was expanded directly into the sample bellow for analysis on the mass spectrometer. Both the sample and reference bellows are compressed to achieve 8e-8 nA current on the major ion beam and were continuously adjusted between each cycle to maintain consistent beam intensity for the full 4 blocks of 20 cycles with no depletion. All seasonally-targeted Δ_{47} samples were replicated three or more times (separate acid reactions), spread out over a period of months to accommodate long-term variation in mass spectrometer behavior. Δ_{47} sclerochronology samples from the Miami shell were each measured a single time in this mode.

In "coldfinger mode", individual aliquots of $CaCO_3$ are much smaller 300–450 µg, but are otherwise treated similarly in the reaction and purification steps. Instead of the (much smaller amount of) pure CO_2 gas being expanded into the bellows, sample gas is frozen into a small coldfinger directly adjacent to the change-over block. Reference gas fills an identical dummy coldfinger on the reference side to a matching pressure, then both are closed and allowed to bleed gradually into the source for 3 blocks of 20 cycles. Pressures (and beam intensities) remain balanced while depleting over the full analysis. Δ_{47} sclerochronology samples from the Colombia shell were each measured a single time in this mode.

 Δ_{47} values were calculated from raw voltages using an R-code script and Brand/IUPAC ¹⁷O parameters, as described in Petersen et al. (2019). Δ_{47} values were projected into the I-CDES90 reference frame by fitting one line through ETH 1 and ETH2 in δ 47 vs Δ_{47} space with a + 0.003% adjustment for the difference between ETH1/2, then using all four ETH standards and defined I-CDES90 Intercarb values (Bernasconi et al., 2021) to create the empirical transfer function. Five in-house standards (calcitic Carrara marble "CM", aragonitic ooids from Joulter's Cay Bahamas "Ooids", an aragonitic coral mixture "CORS", an aragonitic gastropod Cittarium pica "Pica", and a cold-water aragonitic bivalve Arctica islandica "Ice") were run periodically to monitor for drift in corrected values through time. Final Δ_{47} values were converted to temperature using the temperature relationship of Anderson et al. (2021) because it was also anchored to ETH standards. Long-term reproducibility of Δ_{47} is 0.0189‰ (1sd) in "bellows mode" and 0.024% (1sd) in "coldfinger mode", based on ETH and in-house carbonate standard performance over a two-year period.

Carbonate $\delta^{1\hat{8}}O$ values synchronously acquired during analysis of each clumped isotope replicate were combined with the Δ_{47} -derived temperature for the corresponding replicate to calculate replicate/ aliquot-level $\delta^{18}O_w$ values using the water-aragonite fractionation factor of Kim et al. (2007). For seasonally-targeted samples, 3–5 replicates

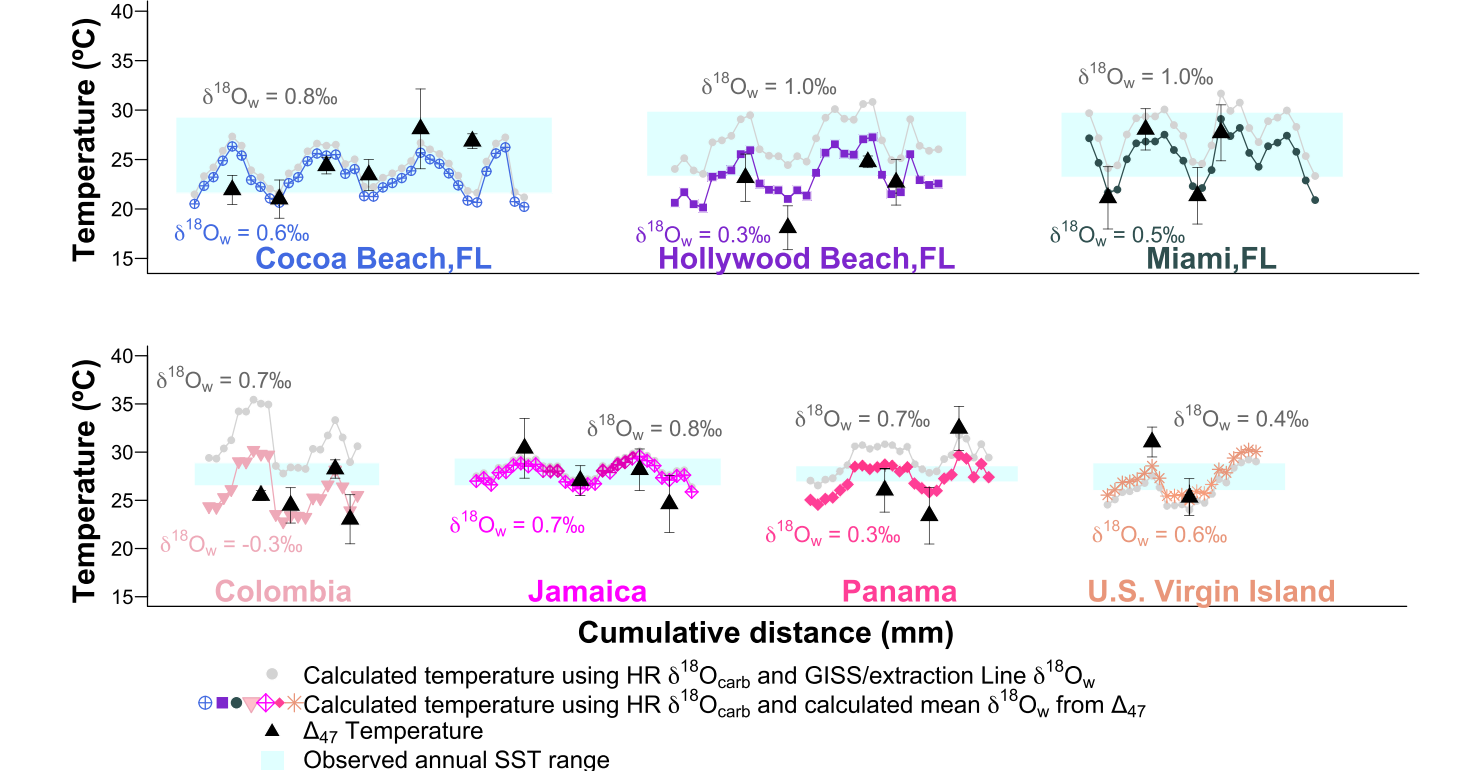


Fig. 4. Reconstructed temperature profiles of seven *L. pensylvanica* shells via different isotope methods. $\delta^{18}O$ sclerochronology converted to temperature assuming constant $\delta^{18}O_w$, using either the mean $\delta^{18}O_w$ calculated from the 2–6 Δ_{47} points shown (colored points) or $\delta^{18}O_w$ measured in modern seawater as part of this study or from the NASA GISS database, whichever was geographically closest (grey points) (Table S1).

were averaged to get a mean $\delta^{18}O,~\delta^{13}C,$ Temperature, and $\delta^{18}O_w$ for each distinct powder. Sample mean values from 2 to 6 seasonally-targeted powders per shell were combined into a shell mean Δ_{47} -derived Temperature and $\delta^{18}O_w$ value. The former was compared to MAT and the later was used to convert subannual-resolution $\delta^{18}O_{carb}$ profiles to temperature profiles assuming $\delta^{18}O_w$ was constant (Fig. 4). The same number of apparent summer and winter points were sampled in most shells, meaning these shell means should not be biased towards one season, with the exception of the Panama shell which had 2 summer and 1 winter. Metrics like standard deviation on these shell averages do not represent uncertainty in the MAT calculation, but instead reflect the magnitude of the seasonal cycle.

For Δ_{47} sclerochronology, aliquot-level δ^{18} O, δ^{13} C, Temperature, and $\delta^{18}O_w$ were combined in two different ways to reduce uncertainty, analogous to the triple replication of homogenous powders employed in seasonally-targeted Δ_{47} samples. In the first method ("smoothing"), a moving window covering N adjacent points was incremented through the whole record to create a smoothed profile (Caldarescu et al., 2021; de Winter et al., 2021), where N=3 or 4 for "bellows mode" (Miami) and N = 4, 5, or 6 for "coldfinger mode" (Colombia) due to their different long-term precisions. In the second method ("optimization"), samples are sorted based on their $\delta^{18}O_c$ values and averages were taken from only the few with lowest $\delta^{18}O_c$ values (supposedly representing the warmest times) or highest $\delta^{18}O_c$ values (supposedly representing the coldest times) regardless of their position in the profile (de Winter et al., 2021). Variable thresholds defining how many points fall into the warm/cold categories were applied, resulting in an increasing number of datapoints being averaged as thresholds approached each other (n = 3or 4; n = 6; n = 8 or 9; n = 10 or 13; Fig. S9–11). A third data treatment method called "binning" has been demonstrated previously for Δ_{47} sclerochronology, where groups of adjacent points are averaged together in bins of varying sizes, guided by the structure of the $\delta^{18}O$ profile (Caldarescu et al., 2021). In that study, a much higher sampling resolution was used. Given our sampling method and the growth rate of L. pensylvanica, we determined that this method was unlikely to be successful in our samples and did not pursue it further.

2.7. Determination of seasonal extrema and inferred growth rate

An age vs. size profile for each specimen was determined from the subannual-resolution $\delta^{18}{\rm O}$ profile, assuming each oscillation from peak to trough represented one year of growth. Although previous studies suggest $\it L.$ pensylvanica spawn in the warm season, 6 out of 7 shells (excluding Miami) show isotope profiles beginning with high $\delta^{18}{\rm O}$ values, inferred to be a colder season. It is likely that if not for the missing exterior layer deferring sampling to 8 mm beyond the umbo, the Miami shell would also show high $\delta^{18}{\rm O}$ values closest to the umbo. Therefore, in all shells the first $\delta^{18}{\rm O}$ minima was assumed to be the first summer and was assigned an age of 0.5 years old. The following $\delta^{18}{\rm O}$ maxima was then assigned to be the first winter at an age of 1 year old. Because shells from different sites lived different lengths of time, growth rates were compared based on length at the second summer.

2.8. Determination of modern seawater $\delta^{18}O_w$

We gathered existing $\delta^{18}O_w$ measurements from the NASA Goddard Institute for Space Studies (GISS) $\delta^{18}O_{sw}$ database (Fig. 1, Table S1) for the study region (5–45°N, 93–42°W) (LeGrande and Schmidt (2006); Schmidt (1999)) (Fig. 1). From this, we selected the closest modern water measurement to each study site, which varied from 34 km away (Miami) to 700 km away (Panama) (Table S1). We supplemented this database with 14 new $\delta^{18}O_w$ measurements from sites in Florida, Atlantic Coast, and Puerto Rico (Table S3). In two cases, newly analyzed water samples provided a closer modern comparison point than was available from the GISS database.

Newly collected seawater samples were analyzed for $\delta^{18}O_w$ in the

University of Michigan Stable Isotope Laboratory using a CO₂-water equilibration method, followed by analysis on a gas-sourced dual inlet mass spectrometer. To prepare samples for equilibration, vials with sealed septa were first flushed and filled with dry tank CO₂ to a head-space pressure of 1 atm. A 4 ml aliquot of sample or standard water was injected into each vial, then left to equilibrate in a 25 °C water bath for at least 48 h. After the equilibration period, pure CO₂ was extracted and dehydrated through repeated stages of cryogenic separation at $-95\,^{\circ}\mathrm{C}$ on a custom-built vacuum extraction line (Fig. S2). Each extracted CO₂ sample was dividing into 3–6 aliquots which were separately flame sealed into Pyrex tubes for storage until analysis. Purified CO₂ was analyzed on a Thermo-Finnegan MAT 253 dual inlet mass spectrometer for at least 3 acquisitions of 12 sample-reference cycles at an m/z 44 beam strength of 16 V.

Samples were run alongside in-house liquid standards which, in turn, were calibrated using USGS standards (USGS 45, 46), which were also run occasionally for validation. At least two aliquots of each unknown sample were measured on the mass spectrometer, spread out over weeks to accommodate variation in mass spectrometer behavior, and remaining aliquots were archived in case a third measurement was needed in the future. All new $\delta^{18} O_w$ values are presented relative to SMOW and can be found in Table S2. Results have a typical uncertainty of $\pm 0.1\%$ based on recurrent analysis of our in-house deionised water standard.

3. Results

3.1. Physical parameters, growth rate, and shell size

Shell structures previously documented by Taylor et al. (2004) were observed under scanning electron microscope (SEM), including crossed-lamellar structures in both the middle- and inner-layers and irregular prisms of the pallial myostracum, confirming assumption of negligible post-deposition alteration (Fig. S4).

According to the age determination based on $\delta^{18}\text{O}$ sclerochronology profiles, 1.5 to 4 years of growth were observed, consistent with a maximum documented lifespan of 5 years (Bigatti et al., 2004). L. pensylvanica from the Florida sites lived 3.5-4 years, while the Caribbean L. pensylvanica lived around 1.5–2 years (Fig. 3). Generally, shell length, width, and weight all increase in proportion, with the exception of the CBFL shell; valve length ranged from 20 mm to 45 mm, width ranged from 25 to 50 mm and weight ranged from 1 g to 15 g (Fig. 3). A piece of the CBFL valve was missing, representing roughly a quarter of its shell area, leading to underestimations of true shell weight. Despite being broken, accurate length and width estimates were still possible (Fig. 3D-E, S4). Regardless of total lifespan, 6 out of 7 shells follow the same length-to-age profile (Fig. 3A, B). The apparent exception here is the shell from Jamaica. This shell was the largest and heaviest of the assemblage, reaching a final length of 45 mm, yet only living 2 years according to the δ^{18} O sclerochronology profile (Fig. 3A,

3.2. δ^{18} O-based temperature reconstructions assuming fixed δ^{18} O_{sw}

 $\delta^{18}{\rm O}$ values varied from around -2.0% to 0.0% for FL shells, while three of four Caribbean shells varied within a smaller range of -2.0% to -1.0% (Fig. S5). The shell from Colombia had the lowest absolute $\delta^{18}{\rm O}$ values, ranging from -3.0% to -1.5% and a range of variability ($\sim\!1.5\%$) more in line with the Florida shells than the other Caribbean shells (Fig. S5).

Agreement with instrumental MAT values was the closest when using $\Delta_{47}\text{-based}~\delta^{18}O_w$ values, leading to 5 out of 7 shells with estimated temperatures within 0.5 °C of instrumental MATs. The other two shells (HBFL and Colombia) showed a slight cold bias, with 1.7 and 1.5 °C offsets from the instrumental MAT values, respectively (Fig. 5). Using instrumental/database $\delta^{18}O_w$ values instead changed MAT values by as much as 5–6 °C in some cases. The greatest discrepancies were seen in

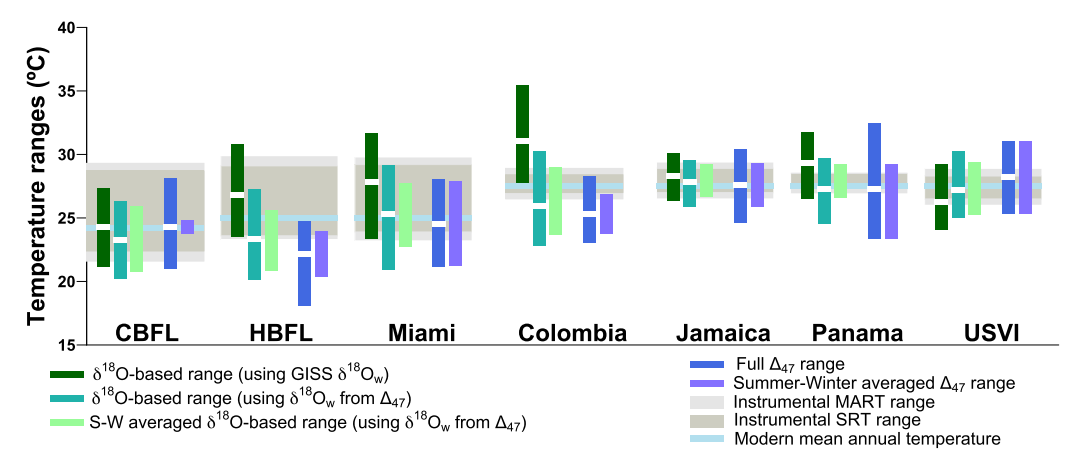


Fig. 5. Range and mean value comparison of reconstructed temperatures via different isotope methods and their comparison with observed seasonality and mean annual temperatures. White bars indicate mean values, calculated as the mean of all temperatures in a given shell profile. S-W = Summer-winter. GISS = Goddard institute for space studies.

sites where the closest available instrumental/database $\delta^{18}O_w$ value was still quite far from the shell collection site (Colombia, Panama, >500 miles away – Table S1). Similarly, estimates of absolute summer and winter temperatures were closer to instrumental values using $\Delta_{47}\text{-based}$ $\delta^{18}O_w$ values.

 $\delta^{18} \text{O-based MART}$ values, which are a function of the magnitude of variability in $\delta^{18} \text{O}$ and not the absolute values, are unaffected by choice of $\delta^{18} \text{O}_w$. Calculated MART values in our 7 shells overestimate true seasonality by $\sim 1-2\,^{\circ}\text{C}$ in most sites. This overestimation in $\delta^{18} \text{O-based MART}$ differs from previous study (Yanes et al., 2012), which suffered from insufficient sampling resolution (Fig. 4-5, S8). MART is significantly overestimated in Colombia (7.4 $^{\circ}\text{C}$ vs. 2.4/1.4 $^{\circ}\text{C}$ MART/SRT) and Panama (5.2 $^{\circ}\text{C}$ vs. 1.8/1.2 $^{\circ}\text{C}$ MART/SRT), potentially indicating a role of seasonally variable $\delta^{18}\text{O}_w$ at these sites, amplifying the fluctuations in $\delta^{18}\text{O}$. Summer/winter averaging reduces the estimated MART by both decreasing summertime estimates and increasing wintertime estimates (Fig. 5). This results in better agreement with instrumental seasonal extremes and MART, potentially due to reduced weighting of outliers or single season extremes.

3.3. Seasonally-targeted Δ_{47} -based temperature reconstructions

Seasonally-targeted Δ_{47} samples generally show warm/cool oscillations in line with expectations based on $\delta^{18}\text{O}$, implying correct identification of the position of seasonal extremes (Fig. 4). An exception to this is the shell from CBFL, which shows a 'stair-step' pattern of temperatures increasing through time, but individual winters still cooler than adjacent summers (see Supplement).

Seasonally-targeted Δ_{47} -based mean annual temperature estimations (averaging n=2–6 samples/shell) result in excellent agreement (within 0.5 °C) with instrumental MAT in 5 of 7 shells, excluding HBFL and Colombia (Fig. 5). Typical methods of determining uncertainty such as taking a standard deviation would reflect the magnitude of the seasonal cycle in a given location as opposed to uncertainty in the average and therefore are not plotted or considered.

 Δ_{47} -based MART reconstructions match true MARTs for the FL sites very well (<0.5 °C offset), but overestimate MART for the Caribbean sites (Fig. S8C). This overestimated MART is most prominent in the Panama shell which estimates a MART 7.1 °C greater than the instrumental MART. When Δ_{47} values from multiple apparent summer or winter zones were averaged prior to calculating a difference, the resulting MART estimate was reduced for all sites except USVI (Fig. 5, Table S2). This improved alignment with instrumental MART for the Caribbean sites but worsened it for Florida sites, CBFL especially (Fig. S8C—D). In the Caribbean sites, MART estimates are reduced by up

to 3.2 $^{\circ}$ C due to summer-winter averaging, yet this is still not enough to match the extremely low MART in these tropical sites (Fig. S8D). Averaging over more summers/winters would likely reduce theses MART estimates further, if shells with longer lifespans could be found from these sites.

 $\delta^{18}O_{W}$ calculated from Δ_{47} are ranged as follows: -0.1 to +1.4%(CBFL), -0.2 to +0.9% (HBFL), 0 to +1.1% (Miami), -0.5 to +0.2% (Colombia), +0.3 to +1.1% (Jamaica), -0.2 to +1.0% (Panama), +0.5to +1.5 ‰(USVI) (Fig. S13). Mean values are within 0.5‰ of instrumental/database values for 5 of 7 sites (Table S1). Larger differences occur where the database value comes from >500 miles from the shell collection site (e.g., Colombia). Mismatch of Δ_{47} -derived and instrumental $\delta^{18}O_{W}$ values from HBFL, which were collected from the exact same site as the shell, may indicate that the few-day period in which the modern waters were collected was not representative of the annual average, or that the beach-collected shell lived during a period where local $\delta^{18}O_w$ values were much different than today. Absolute $\delta^{18}O_w$ values depend heavily on the choice of δ¹⁸O_w-Temp-CaCO₃ calibration, for which there remains uncertainty in the aragonite-water system sufficient to explain the rest of the observed offsets (Zhou and Zheng, 2003; Kim et al., 2007).

3.4. High resolution Δ_{47} temperature reconstructions - optimization

The "optimization" method of processing Δ_{47} sclerochronology data returned very different results in the two shells analyzed. In the Colombia shell, estimates of summer and winter temperature were consistently close to each other, in line with the small instrumental MART at this site. Absolute MART (and uncertainty) decreased as thresholds were brought closer together and more points were averaged on either extreme (Fig. 7, Figs. S10–12). The best estimate of MART was achieved by averaging the top 13 points and the bottom 11 points, which corresponds roughly to the top and bottom halves of the data (n=5 points excluded in the middle) (Fig. 7). However, selecting such a large fraction of the data goes against the idea of isolating seasonal extremes. Averaging a randomly selected 13 points and 11 points resulted in a MART of \sim 3 °C.

In the Miami shell, estimates of summer and winter temperatures and MART were similar regardless of thresholds used (<3 $^{\circ}\text{C}$ variation in either extreme). However, all ranges were reversed from expectation, with the low $\delta^{18}\text{O}$ points corresponding to the colder temperature and vice versa. $\delta^{18}\text{O}$ values for the first four points of the sclerochronology profile disagreed between original $\delta^{18}\text{O}$ sclerochronology and $\delta^{18}\text{O}$ values acquired during H.R. Δ_{47} analysis, potentially leading to misassignment into a seasonal average using the optimization method

(Fig. S6). Removing these four points reduced the reconstructed MART, but all ranges remained reversed (Fig. S12).

3.5. High resolution Δ_{47} temperature reconstructions - smoothing

In the Miami shell, the smoothing method estimated Δ_{47} values from 0.57 to 0.60% using a window size of n=3, equivalent to a temperature range of 21.9 to 31.9 °C. This range is greater and temperatures are warmer than those estimated based on seasonally-targeted Δ_{47} points of 0.59 to 0.61% (temperatures of 21.1 to 28.1 °C) (Table S2). This is also warmer than the instrumental MART of 23.2–29.8 °C, although it is well-centered. The mean H.R. Δ_{47} temperatures for the Miami shell is estimated to be 27.2 °C compared to the instrumental MAT of 25.0 °C. This slight positive bias may be the result of preferential growth during warmer months, leading to a volumetric weighting towards warmer temperatures when all equally-spaced points are combined. Comparing the midpoints of the estimated ranges leads to an even closer agreement (26.9 for H.R. Δ_{47} range vs. 26.5 for the instrumental range).

The structure of the "smoothed" record appears to align with the $\delta^{18}O$ reconstructed record. Low $\delta^{18}O$ zones occurring around 15-17 mm, 28-30 mm and 35-40 mm (Fig. 4, Fig. S5, Fig. 6A) roughly correspond to low Δ_{47} zones around 17 mm, 28 mm, and 35 mm (Fig. 7B, Fig. S5), with similarly aligning high $\delta^{18}O$ and high Δ_{47} zones in between. Around 8-10 mm, Δ_{47} values are also low, which aligns with another low $\delta^{18}O$ zone in the $\delta^{18}O$ reconstructed record (Fig. S5, Fig. 4). Re-drilled powders from this early portion surprisingly showed higher $\delta^{18}O$ values during H.R. Δ_{47} analysis, potentially due to drilling into different layers (Fig. S6).

 $\delta^{18}O_w$ values estimated from data smoothing range from -0.3 to +2.2%, with a mean of 0.9%, which matches closely to the instrumental/database value of 1.0% (Table S1). This differs from the mean $\delta^{18}O_w$ value from seasonally targeted Δ_{47} of 0.5%. No coherent seasonal signal is observed aligning variation in $\delta^{18}O_w$ with identified seasonality in temperature. The $\delta^{18}O_w$ record is particularly invariant across the last two years of growth.

In the Colombia shell, increasing the window size reduced the estimated MART from 15.6 to 11.6 (Table S2). However, even with a window size of n=6, the calculated temperature range of 21.7 to 33.3 °C is still much larger than the range estimated from seasonally-targeted Δ_{47} measurements (23.0 to 28.3 °C) or from the instrumental record (26.5–28.9 °C) (Figs. 6, 8). Despite this large overestimation in temperature range, the mean H.R. Δ_{47} temperature is well centered.

The shape of the δ^{18} O reconstructed record suggests two years of growth indicated by two summer peaks occurring around 8-10 mm and 20-22 mm and two winter peaks around 12-15 mm and 25 mm. In contrast, the H.R. Δ_{47} smoothed temperature record suggests one year of growth, indicated by a single "plateaued" summer extreme peaking around 10 mm and a single winter extreme occurring around 20-22 mm (Fig. 6, S6). Given the small Colombia shell size (25X25mm), the 1-year growth estimated from H.R. Δ_{47} may be more reasonable. Assuming one year of growth, the adjusted growth rate of the Colombia shell would match those of the USVI shell, which lived for 1.5 years with a shell size of 21X25mm (Fig. 3).

 $\delta^{18}O_w$ values estimated from data smoothing range from -0.8 to +1.7% in the Colombia shell, with a mean of 0.5% (Fig. 6F). This differs from the mean $\delta^{18}O_w$ value from seasonally targeted Δ_{47} of -0.3%, which was used to convert $\delta^{18}O$ sclerochronology to temperature in Figs. 4 and 5, and the instrumental/database value of 0.7%. If $\delta^{18}O$ sclerochronology was converted to temperature using 0.5%, this would result in absolute temperatures closer to those estimated using the instrumental value. This is complicated by the fact that we observed a 0–0.5% offset between $\delta^{18}O$ values measured during $\delta^{18}O$ sclerochronology and both H.R. Δ_{47} analysis (Fig. S6) and seasonally targeted Δ_{47} analysis. Depending on which of these is more accurate, this could shift estimated $\delta^{18}O_w$ values by a similar amount and the subsequent $\delta^{18}O$ -based temperatures by 0–2 °C.

4. Discussion

4.1. Consistent growth rates and shell morphology, with a few exceptions

 $L.\ pensylvanica$ shells from all sites appear to follow the same length-to-age growth curve, which is also consistent with previous studies (Bigatti et al., 2004) (Fig. 3A). The sole exception is the shell from Jamaica, which grew bigger, faster (Fig. 3A). Weight is also elevated in this specimen relative to length and width (Fig. 3D,E), indicating a thicker shell relative to others. The Jamaica site has one of the warmest mean annual temperatures of any site from this study, which may explain this prolific growth, yet Panama and Colombia have similarly warm climates but demonstrate 'regular' growth. After revisiting the growth curve for the Colombia shell to reflect 1 year of growth instead of 2 based on the Δ_{47} sclerochronology data (smoothing), the inferred higher growth rate is larger than most other shells but still less than Jamaica.

After accounting for the missing outer layer in the first 8 mm of the Miami shell, all new $\delta^{18}{\rm O}$ profiles begin with high $\delta^{18}{\rm O}$ values, indicating a winter start to shell growth. At first, this seems to contradict the early studies that show warm season spawning (Bigatti et al., 2004; Taylor et al., 2004; Yanes et al., 2012). We interpret these new results to suggest that following spawning, a measurable thickness of shell does not accumulate until the first winter season. Sampling nearest the umbo is either not close enough to the peak of the umbo to sample the true start of growth, or drilled too deeply, combining shell accreted in the first warm months with subsequent cooler months.

Shells from our study show a roughly 1:1 ratio of length to width (Fig. 3F). This is consistent with a L. pensylvanica population from the Bahamas (Yanes et al., 2012), but another population from FL Keys (Taylor et al., 2004) show greater length to width, or a more elongated as opposed to circular shell shape. It's possible that this discrepancy is due to different methods of measuring width, although the magnitude of the difference (\sim 10 mm) seems too great for this explanation, given the circularity of the shells. If real, this may suggest population-scale morphological change.

4.2. Temperature reconstructions assuming fixed $\delta^{18}O_{sw}$

Typical studies employing $\delta^{18} O\text{-based}$ paleothermometry usually assume a constant $\delta^{18} O\text{w}$ value (Schöne et al., 2004; Jones et al., 2005). However, without accurate knowledge of $\delta^{18} O\text{w}$, the converted maximum and minimum temperatures, and MATs can be skewed in either direction. This is demonstrated through $\delta^{18} O\text{-based}$ temperature ranges calculated using the GISS database $\delta^{18} O\text{w}$ value, which is representative of a "best guess" modern estimate that might be used in a paleoclimate study. Temperatures estimated using database $\delta^{18} O\text{w}$ values are both too high (Colombia) and too low (USVI). Best alignment with MAT and summer/winter temperatures was achieved when the selected $\delta^{18} O\text{w}$ value was located close to the shell collection site. The agreement deteriorates as the selected $\delta^{18} O\text{w}$ values were recorded farther away from shell collection site, like in Colombia and Panama (Fig. 5, Table S1).

Better agreement in MAT and MART estimates with instrumental values was achieved when using $\Delta_{47}\text{-based}$ shell mean $\delta^{18}O_w$ values, which should reflect a highly localized estimates of $\delta^{18}O_w$, therefore more accurate than database values. This indicates at least one method of estimating $\delta^{18}O_w$ using Δ_{47} analysis should be conducted in all paleoclimatology studies. In increasing order, a single bulk Δ_{47} analysis (drilled to average over a large portion of the shell), the mean of multiple seasonally-targeted Δ_{47} analysis, or the mean of continuous H.R. Δ_{47} analyses should be used to convert H.R. $\delta^{18}O$ values into a record of seasonal temperature variability.

However, all of these approaches still assume seasonally invariable $\delta^{18}O_w$, which may not be the reality in some environments. This is reflected through observation that $\delta^{18}O\text{-based}$ MART estimates in Colombia, Panama and USVI that assume constant $\delta^{18}O_w$ overestimate

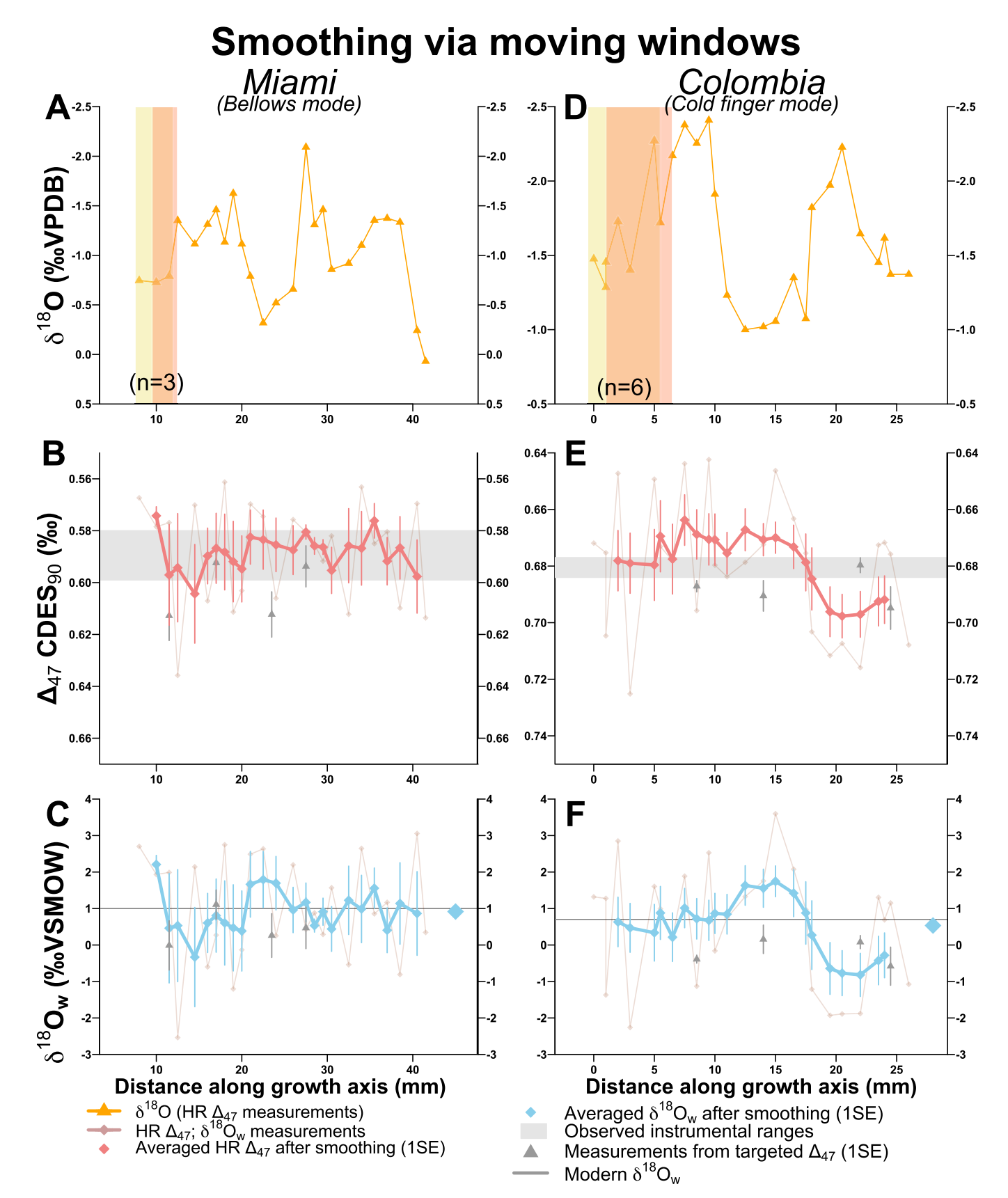


Fig. 6. A, D. δ^{18} O measurements from stable isotope and H.R. Δ_{47} -based thermometry. B, E. H.R. Δ_{47} measurements and averaged datapoints after data smoothing via a moving window (1SE). Grey points show seasonally-targeted Δ_{47} measurements. C, F. δ^{18} O_w derived from H.R. Δ_{47} measurements and averaged datapoints after smoothing (1SE). Grey points show δ^{18} O_w derived from seasonally-targeted Δ_{47} measurements.

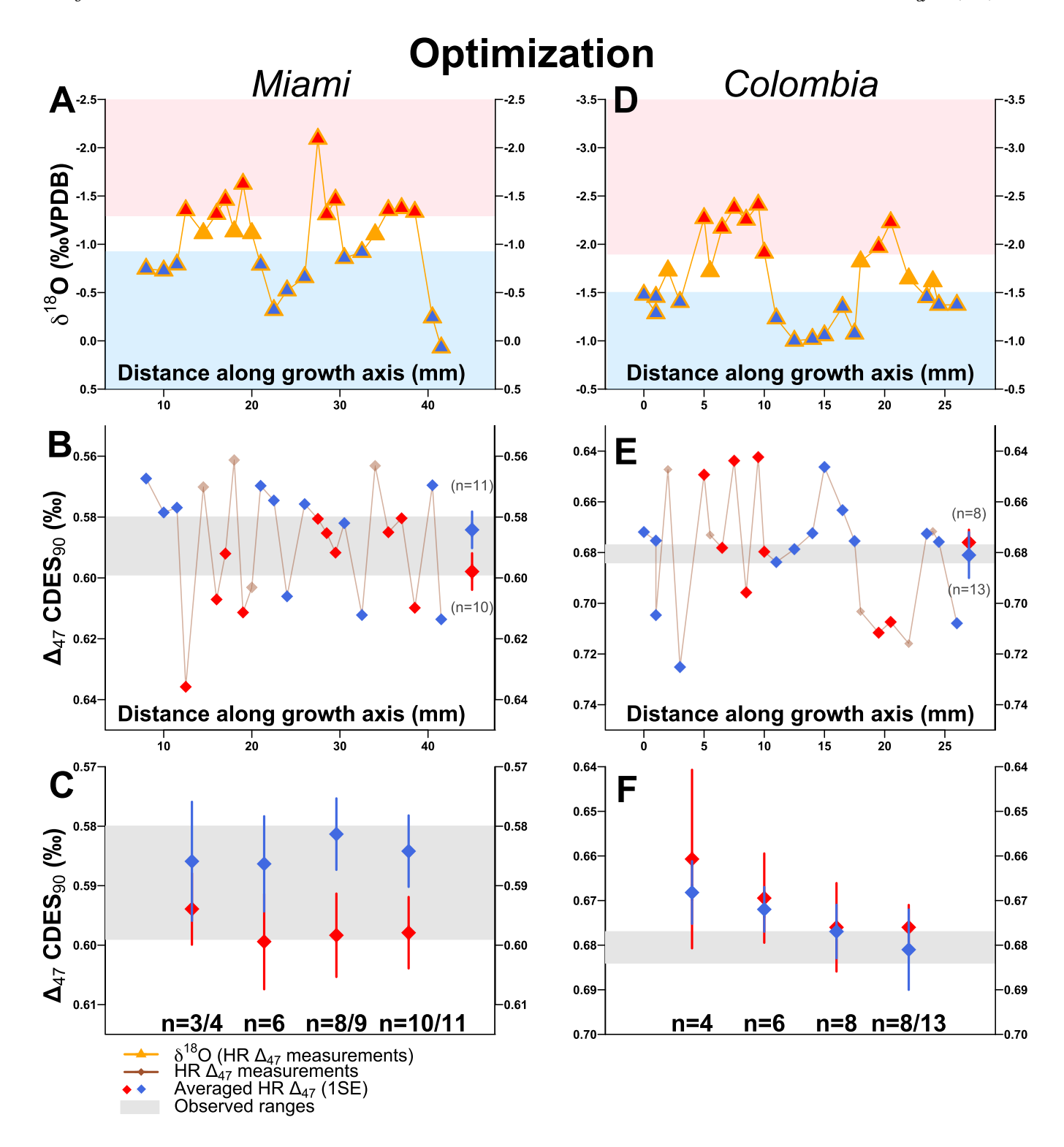


Fig. 7. A, D. δ^{18} O measurements from stable isotope and H.R. Δ_{47} -based thermometry. Pink and blue shading indicates warm and cold thresholds defined based on data optimization. B, E. H.R. Δ_{47} measurements with red and blue colored datapoints plotted based on thresholds selected using data optimization. C, F. Averaged Δ_{47} values from each of repeated optimization approaches with different numbers of datapoints combined. (For interpretation of the references to colour in this figure legend, the reader is referred to the web version of this article.)

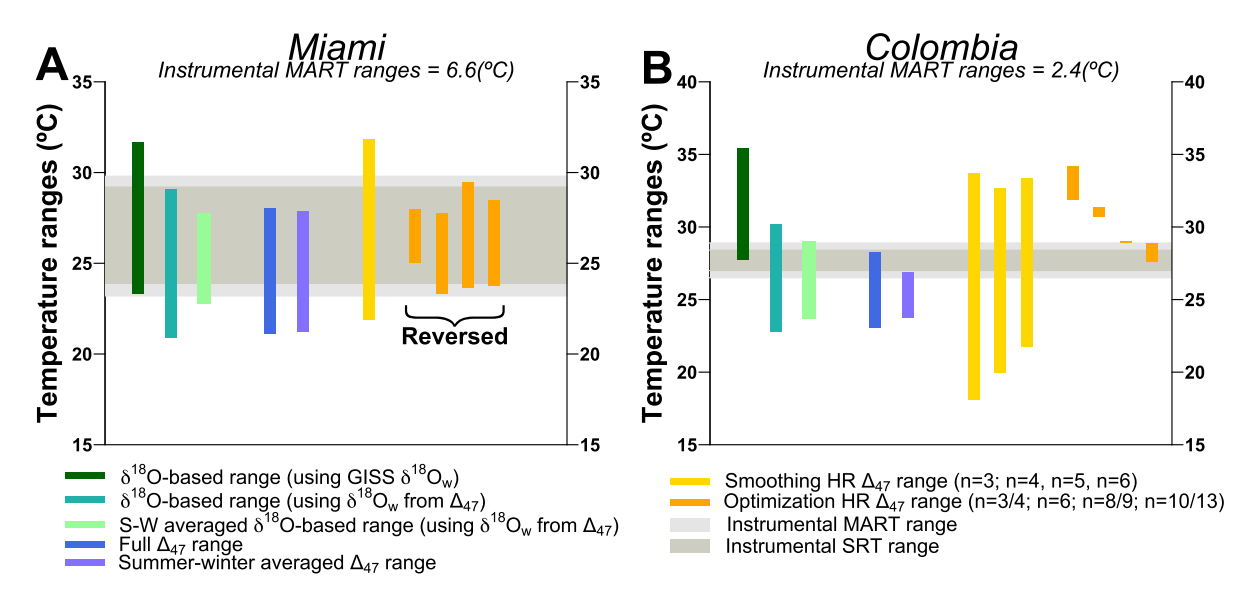


Fig. 8. Summary of reconstructed temperature ranges using different approaches and comparison against observed seasonality (grey shading). Note that the Miami shell was analyzed under bellows mode while the Colombia shell was analyzed under coldfinger mode for H.R. Δ_{47} measurements.

instrumental MARTs by up to 5 °C, likely indicating seasonally variable $\delta^{18}O_w$, which is amplifying the fluctuations in $\delta^{18}O$. In the sections below, we discuss two cases differently effected by seasonally variable $\delta^{18}O_w$ from this study.

4.3. Seasonally variable $\delta^{18}{\rm O}_{\rm w}$ and moderate temperature seasonality: Miami

Seasonally-targeted Δ_{47} measurements for the Miami shell follow the expected pattern of warm/cool oscillation, with apparent summer intervals (δ^{18} O minima) tending to produce warmer temperatures than those targeting apparent winter intervals (δ^{18} O maxima), implying correct identification of seasonal extremes and limited variability in δ^{18} O_w. However, δ^{18} O-based MART estimates slightly overestimate true MART, suggesting δ^{18} O_w is in fact varying and that variation amplifies the δ^{18} O range. To achieve amplification of the δ^{18} O range, the highest (lowest) δ^{18} Ow values must occur during the coldest (warmest) times.

H.R. Δ_{47} analysis with data smoothing, producing subannual temperature and $\delta^{18}O_w$ records, is independent of any assumptions about seasonal timing or magnitude of $\delta^{18}O_w$ variability, or a priori assignment of the position of summer/winter shell growth. This method does a very good job capturing true seasonality over multiple years (Fig. 6). This appears worse in the absolute range (Fig. 5) due to single-point extrema that lie outside of the true range. However, Fig. 6 clearly shows that for three of four years of growth, the summers and winters align well with instrumental temperatures. This suggests that summer/winter averaging of the smoothed record would perhaps result in the best estimate of seasonal temperature extremes and MART.

Supporting above inferences that $\delta^{18}O_w$ is varying, the continuous $\delta^{18}O_w$ profile calculated from seasonally targeted Δ_{47} shows variation of $\sim\!1.1\%$, although error bars are large. There is no coherent seasonal signal in this $\delta^{18}O_w$ profile. The first two years contain most of the variability, whereas the latter two years are relatively invariant. Variability of $\sim\!0.6\%$ in $\delta^{18}O_w$ near Miami have been observed in a short 1.5-year-long record from 1989 to 1991 (Leder et al., 1996), and measured $\delta^{18}O_w$ extrema similarly did not show any coherent seasonal pattern. This suggests that this record is accurately capturing real (highly variable) patterns of $\delta^{18}O_w$ variability around Miami.

Although H.R. Δ_{47} measurements with data optimization appears to capture the MART and absolute seasonal extremes well, the summers and winters are reversed (Fig. 7-8). When $\delta^{18}O_w$ values are varying unpredictably at the subannual scale as suggested above by both

instrumental measurements and H.R. Δ_{47} with data smoothing, using absolute thresholds for $\delta^{18}O$ values can be inaccurate because $\delta^{18}O$ values of seasonal extremes may not always be the same. This is particularly apparent in the wintertime $\delta^{18}O$ values in the Miami shell, which vary from 0 to -1.3%.

Overall, in a situation with unpredictable, highly variable $\delta^{18}O_w$ patterns, H.R. Δ_{47} with data smoothing works very well. Both $\delta^{18}O_b$ based methods assuming fixed $\delta^{18}O_w$ and H.R. Δ_{47} with optimization which assumes correct identification of seasonal extremes perform worse and are not recommended.

4.4. Seasonally variable $\delta^{18}{\rm O_w}$ and low temperature seasonality: Colombia

 $\delta^{18}O\text{-}based$ MART estimates assuming constant $\delta^{18}O_w$ significantly overestimate true MART in tropical Colombia (Fig. 4), suggesting high variability in $\delta^{18}O_w$ throughout the year. This could possibly be occurring in-phase with temperature changes (highest $\delta^{18}O_w$ during coldest months and vice versa), amplifying the apparent seasonal cycle in $\delta^{18}O$. However, due to the extremely low true MART in Colombia, even moderate $\delta^{18}O_w$ variability could falsely create an apparent seasonality in $\delta^{18}O$ that would lead to misidentification of seasonal extremes. If $\delta^{18}O_w$ cycled from lower to higher values multiple times within a single year, this could result in a $\delta^{18}O$ record suggesting more years of growth than in fact occurred.

Misidentification of seasonal extremes in the $\delta^{18}O$ record is supported by multiple lines of evidence. Seasonally-targeted Δ_{47} show a confused pattern in the Colombia shell, with one of the most glaring mismatches with expected seasonality occurring in the first "summer" sample (Fig. 4). H.R. Δ_{47} with data smoothing suggests only one instead of two years of growth, with the summer aligning with a $\delta^{18}O$ minima (as precited), but the winter aligning with the second $\delta^{18}O$ minima (previously inferred to be a second summer). This divergence in the number of years of growth suggests $\delta^{18}O_w$ cycling more than once per year, but this is not reflected in the smoothed H.R. Δ_{47} -based $\delta^{18}O_w$ record, which shows highest values in the fall season and lowest in the winter season (-0.8 to +1.7%).

There is substantial evidence supporting $\delta^{18}O_w$ variability in Colombia. Colombia has the second highest seasonal variation in precipitation (SVP) of any of our sites, experiencing 219 mm difference in monthly rainfall between the wettest and driest month. The rainy season, which would deliver precipitation that was depleted in heavy

isotopes compared to seawater, occurs during the warm season of May–October, with dual peaks in May and October and very dry conditions conducive to evaporative enrichment in January–March (Fig. S1). In addition to the local rainfall, the Dique Canal discharges 55–250 $\rm m^3/s$ freshwater from the greater Magdalena River watershed into Cartegena Bay, driving significant salinity gradients of $\sim\!30$ psu between surface and bottom waters and $\sim\!10+$ psu variations in surface waters between the rainy seasons and dry season (Tosic et al., 2019). The timing of discharge is slightly delayed from local rainfall, with two peaks in June–July and November–December, and lowest values in February–April. Taken together, this complicates predictions of the exact timing of $\delta^{18}{\rm O_w}$ variability, but suggests a complex pattern of subannual $\delta^{18}{\rm O_w}$ variability is highly plausible.

Surprisingly, despite the apparent inaccuracy of seasonal identification based on δ^{18} O, it appears H.R. Δ_{47} measurements with data optimization achieved best agreement with observed seasonality for the Colombia shell. Particularly with an increased window size, averaging the top 13 points and the bottom 11 points, the calculated range becomes perfectly aligned with its small instrumental MART (Fig. 7). This is the only method to result in such a low MART. However, this is likely due to larger number of datapoints being combined here rather than superior data combination strategy. When only averaging 3-4 datapoints, the optimized H.R. Δ_{47} MART estimated for the Colombia shell was much warmer than its instrumental MART. When true seasonality is low, averaging any half of the points will result in a value close to the MAT. The alignment of the summer, as inferred from smoothed H.R. Δ_{47} , with the first low δ^{18} O peak around 5-10 mm likely kept the inferred summer temperature above the inferred winter temperature using any thresholds.

In a situation where $\delta^{18}O_w$ varies multiple times per year, using any method that requires assigning position of seasonal extremes using the $\delta^{18}O$ record is a poor choice. This is especially true in a location with low temperature seasonality. (If temperature seasonality was high, such as in a mid-latitude site, temperature seasonality could overprint low to moderate $\delta^{18}O_w$ variability and still result in correct seasonal identification.) Although the H.R. Δ_{47} with smoothing should have given us the best results, this method still overestimated MART significantly, perhaps due to increased uncertainty in coldfinger mode. Despite the

overestimation in MART, the mean of all H.R. $\Delta_{\rm 47}$ points best matches MAT.

4.5. Choosing the best method: Sample size vs. growth rate vs. analytical resolution

A single measurement of Δ_{47} , un-replicated, has a large uncertainty which is mostly a function of integration time. The two measurement modes on the Nu Perspective used in this study ("bellows mode" for 3-4 mg aliquots and "coldfinger (CF) mode" for 300-400 μ g aliquots) have different single-replicate uncertainties due to different integration times (80 vs. 60 cycles, respectively), best quantified by the long-term standard deviation of carbonate standards (sd = 0.018% for bellows mode, sd = 0.024% for CF mode). On a Kiel device (as used by de Winter et al., 2021), a single replicate of 80-250 µg only runs for 20 cycles, resulting in larger single-replicate uncertainty (long-term 1sd = 0.04%). These uncertainties are reduced in the ultimate sample mean through replication. Depending on which of these methods are used, a different number of replicates are needed to achieve a temperature estimate with a desirably low uncertainty of $\sim 1-2$ °C, equivalent to $\sim 0.010\%$ 1SE in Δ_{47} at Earth surface temperatures. In bellows mode, 3-4 replicates are needed, compared to 5-6 for CF mode and 15-18 for Kiel-based measurements. On average, temperature error on a sample with >3 replicates measured in bellows mode is about 2–3 $^{\circ}$ C.

When sampling for H.R. δ^{18} O or Δ_{47} sclerochronology, the physical sampling resolution is limited by the size of the drill bit and the spacing between drilled points, regardless of the total shell size or annual growth rate. Assuming sampling is conducted with essentially no spacing between each sample point, the maximum number of points per unit distance along the growth axis is defined by the width of the drill bit alone (e.g. with a 1 mm drill bit, you can achieve 1 point per mm). To go to even higher resolution, "trough sampling" can be used, where the drill bit shaves off a thin slice of material that is thinner than the drill bit width, leaving behind a trough. This trough sampling results in less powder per point as the distance along the growth axis is smaller, so widening of the trough from side to side, tracing growth bands, ("lateral extension") is often needed to acquire enough material. This is often done with a micromill, which uses a computer-controlled drill to

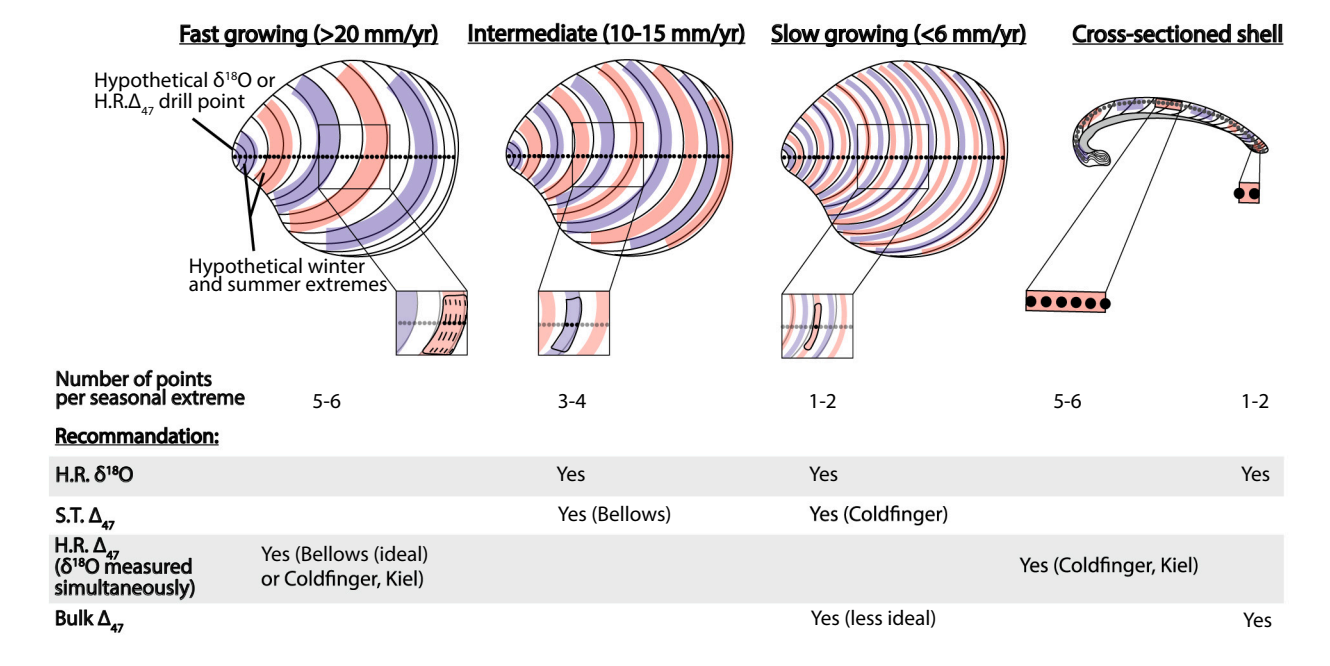


Fig. 9. Diagram showing relation between growth rate and analytical resolution with recommended isotope techniques. H.R. = High Resolution; S.T. = Seasonally Targeted.

carefully drill out designated pathways. Lateral extension is only possible when sampling the top surface of the shell where growth bands are visible and is not possible when drilling on the interior surface of a cross sectioned shell (Fig. 9). Lateral extension can also be used to acquire larger amounts of material for more material-intensive methods like bellows mode.

Growth rate, total lifespan and shell size should be considered when selecting the most effective clumped isotope sampling approach. Growth rate (mm along growth axis per year of life) translates points per unit distance into points per unit time (e.g. points/year of growth). More importantly for the purposes of seasonality estimation, the growth rate combined with the sampling resolution defines the number of points per seasonal extreme. In order to capture the full magnitude of seasonal variability, a resolution of >1 point per month must be achieved, whether for δ^{18} O or H.R. Δ_{47} analysis. If shell growth rates are too slow, a single drill hole will combine material from multiple months of growth and produce a seasonal average instead of a warmest or coldest month mean. Total shell size defines the ability to extend drill points laterally to acquire more sample powder from a similarly narrow unit of time/distance. Total lifespan determines the number of years of growth that can potentially be averaged together, such as in the summer-winter averaging method.

In the above study, we demonstrated that H.R. Δ_{47} with data smoothing produces the best estimates of absolute summer and winter temperatures and MART because this method 1) does not assume the position of seasonal extremes; 2) does not assume that $\delta^{18}O_w$ is constant throughout the year; and 3) does not require prior knowledge of the mean $\delta^{18}O_w$ value. However, in order to achieve robust temperature estimates for seasonal extremes and MART, enough points per seasonal extreme must be sampled and averaged together. Depending on the analytical methods used, at least 3 replicates/aliquots and possibly as many as 20 replicates/aliquots must be averaged. This may not be achievable if growth rates are too slow, drill bit and/or point spacing is too large, or shell size is too small. Fig. 9 describes the recommended oxygen and clumped isotope sampling approach for different shell growth rates.

In fast growing shells (>20 mm/yr), sampling resolution of \sim 1 mm between points (such as that achieved in this study using a hand drill) will easily result in 12–20 pts. per year, 1–2 points per month, or 4–6 points per season. In this regime, we recommend H.R. Δ_{47} sampling for bellows mode with smoothing, acquiring 3-4 mg single aliquots along the whole transect, using lateral extension and growth band tracing to acquire enough material per aliquot. In bellows mode, a smoothing window of n=3 is sufficient, which under this high growth rate scenario would combine material from at most 2 adjacent months, capturing seasonal extremes well. H.R. Δ_{47} with smoothing using CF mode would also be possible, as a smoothing window of n=6 would still likely be able to capture a single season average, but not the single warmest or coldest month by itself. This is demonstrated by the Colombia shell (Fig. 6). CF mode becomes increasingly applicable as growth rates increase.

In a shell with an intermediate growth rate (10-15 mm/yr), sampling resolutions of $\sim\!1$ point per month, or $\sim\!3$ points per seasonal extreme would still allow H.R. Δ_{47} with smoothing using bellows mode, where the window size of n = 3 would capture a seasonal extreme but not quite the single warmest/coldest month. This is demonstrated by the Miami shell (Fig. 9). H.R. Δ_{47} with smoothing using CF mode would not be a good choice for slower growing shells, as the larger window size would necessarily combine aliquots from shoulder seasons, resulting in muted estimates of MART. If growth rates get slower than this, there are insufficient points per month or points per season for H.R. Δ_{47} methods.

When growth rates are intermediate (10-15 mm/yr) or slow (<6 mm/yr) and H.R. Δ_{47} methods are not possible, seasonally-targeted Δ_{47} approach combined with H.R. $\delta^{18}O$ sclerochronology can substitute. Although this method requires proper identification of seasonal extremes from $\delta^{18}O$ profiles, by averaging many replicated Δ_{47} samples

from across the shell, mean $\delta^{18}O_w$ values and MAT estimates become more robust. Whether $\sim\!1\text{--}2$ points per seasonal extreme (slow growth) or $\sim 3\text{--}4$ points per seasonal extreme (intermediate growth) are achieved in $\delta^{18}O$ sclerochronology, a single homogenous powder can be drilled from the appropriate growth interval, with lateral extension tracing the growth band if needed to increase material acquired. Depending on the thickness of the growth interval in question and limitations on lateral extension due to total shell size or preservation, this could be $\sim\!12\text{--}15$ mg replicated 3–4 times in bellows mode (as demonstrated in all 7 shells, Fig. 9) or $\sim\!2$ mg replicated 5–6 times in CF mode. In smaller shells, tracing growth bands laterally without risking drilling into other layers may be more difficult, favoring CF mode.

If lateral sampling is too difficult due to small shell size or poor exterior preservation, seasonally-targeted Δ_{47} sampling can be replaced with a single bulk Δ_{47} sample. Preferably, this is done by drilling a long transect along the growth direction or a wide hole near the ventral margin, both intended to average multiple years of growth. Some organisms shut down growth during certain seasons, so this bulk measurement may not necessarily represent mean annual conditions. This can often be determined from δ^{18} O profiles.

Lastly, $\delta^{18}O$ sclerochronology is routinely conducted on a cross-sectioned shell because growth bands are most visible from this view. When sampling the exterior, we extended our drill spots laterally, following a curved path delineated by growth bands to capture more material while limiting time averaging. However, when drilling into the cut face, lateral extension like this is impossible because curvature of growth bands from the center to the edge of the shell is hidden within the shell interior and the risk of drilling into adjacent growth intervals is great. In this case, HR Δ_{47} with CF mode can acquire both $\delta^{18}O$ and Δ_{47} sclerochronology (Fig. 9). If growth rates are high enough, such as in the younger portion of some shells, data smoothing with CF mode may be able to estimate warmest/coldest month, or seasonal extremes. If growth rates are slower, overall or towards the ventral margin, H.R. Δ_{47} with smoothing will not work, as in the slow growing shells described above. Here, we suggest bulk Δ_{47} combined with $\delta^{18}O$ sclerochronology.

Kiel-derived Δ_{47} sclerochronology requires many more aliquots per season to work properly, but each aliquot can be smaller. This is conducive to "trough sampling" often drilled via micromill, where very small aliquots can be acquired with confidence. A recent study by Caldarescu et al. (2021) conducted high resolution Δ_{47} -based sclerochronology with similar data averaging strategies, with very small aliquots analyzed using a Kiel device. The bivalve used (*Megapitaria aurantiaca*) was much larger and faster growing compared to *L. pensylvanica*, ranging from 50 to over 100 mm in length, providing more surface area for higher resolution sampling (López-Rocha et al., 2021). They averaged together anywhere from n=14 to n=61 points per season. As in our study, they were able to achieve good agreement with instrumental temperatures.

Taken together, any of the analytical methods can be used (bellows, CF mode, or Kiel-based Δ_{47}), but the variable precision of these methods must be balanced against sampling resolution, growth rates, and shell size (Fig. 9). In this way, our results from *L. pensylvanica* can be generalized for any bivalve species.

5. Conclusions

In this study, we applied multiple isotope techniques to modern L. pensylvanica collected from seven locations, spanning $\sim\!20^\circ$ in latitude, to assess their ability to correctly record mean annual temperatures and seasonality and to establish the most reliable sampling approach and data treatment method for paleotemperature/paleoseasonality reconstruction. Altogether, we did not observe any seasonal, mean temperature, or biologically-induced (species-specific) biases in modern L. pensylvanica, suggesting species from within the same genus and/or family could serve as reliable paleotemperature/paleoseasonality recorders for future work.

 $\delta^{18} \text{O-based}$ reconstruction of MART best matched modern MART, especially after averaging multiple summers and winters. However, without knowing the regional $\delta^{18} \text{O}_w$ values, $\delta^{18} \text{O-based}$ reconstructions do not accurately capture absolute summer and winter temperature extremes. This can be improved using a seasonally-targeted $\Delta_{47}\text{-based}$ sampling approach. Yielding sub-annual scale $\Delta_{47}\text{-temperatures}$ as well as $\delta^{18} \text{O}_w$ values, this approach allows for seasonal variations in $\delta^{18} \text{O}_w$ and produces more reasonable max-to-min ranges and the best estimates of MAT.

The best method for reconstructing MAT, MART and absolute seasonal temperature extremes while allowing for and directly quantifying variability in $\delta^{18}O_w$ is H.R. Δ_{47} with data smoothing. This method removes the need to assign the position of seasonal extremes based on the δ^{18} O profile. However, in order to effectively apply H.R. Δ_{47} -based reconstructions, a delicate balance must be struck between analytical method used, physical sampling resolution, shell size and growth rate. Ideally a minimum of 3–4 Δ_{47} aliquots per season should be drilled for this approach and analyzed using bellows mode for best precision, as demonstrated in the Miami shell. Using the coldfinger mode can reduce the amount of total powder needed for analysis, but much higher sampling resolutions (6+ per season) are needed to overcome the lower reproducibility of this analytical mode. L. pensylvanica is not well suited for this type of approach due to its smaller size and slow growth rate, as demonstrated by the Colombia shell. Larger, faster growing shells should be selected for best estimation of subannual temperatures using H.R. Δ₄₇.

For species with slow to intermediate growth where H.R. Δ_{47} with data smoothing may not be possible, we suggest different sampling methods. Summer/winter averaged seasonally-targeted Δ_{47} -based reconstruction coupled with summer-winter averaged δ^{18} O-based reconstruction using Δ_{47} -derived δ^{18} O_w values are recommended for estimating seasonality and MATs in this situation. Data optimization should only be applied when δ^{18} O_w is independently known to be constant. In the slowest growing shells, a single bulk Δ_{47} sample combined with δ^{18} O sclerochronology can provide a better constraint on δ^{18} O_w than database δ^{18} O_w values, and lead to better absolute seasonal temperature estimates derived from δ^{18} O.

Our results on *L. pensylvanica* can thus be generalized to all bivalves to dictate ideal sampling approaches. This study, combined with other recent studies (de Winter et al., 2021; Caldarescu et al., 2021; Agterhuis et al., 2022) increasingly demonstrate the power of using clumped isotopes at the subannual scale. Subannual paleoclimate data can provide new insight into the more tangible effects of climate change beyond changes in mean annual temperature.

Declaration of Competing Interest

The authors declare the following financial interests/personal relationships which may be considered as potential competing interests:

Jade Z. Zhang reports financial support was provided by National Science Foundation. Sierra V. Petersen reports financial support was provided by National Science Foundation. Sierra V. Petersen reports financial support was provided by Alfred P Sloan Foundation.

Data availability

Coinciding with publication, all raw clumped isotope data will be deposited in the EarthChem ClumpDB database for long-term storage, data DOI: 10.26022/IEDA/112519 (https://doi.org/10.26022/IEDA/112519)

Acknowledgements

We thank Lora Wingate, Steven Wedel, Kyger C. Lohmann, Ashling Neary and Justin VanDeVelde for isotope laboratory assistance at the University of Michigan. We thank S.T. Petersen, S.Wedel, R. Dzombak, M. Mustafa and the University of Michigan department of Earth and Environmental Sciences for crowd-sourcing shell collection. This project was supported by National Science Foundation grant 1903237, Alfred P. Sloan Research Fellowship to S.V. Petersen, National Science Foundation GRFP, Rackham Graduate School Merit Fellowship and University of Michigan Turner Grant to J.Z. Zhang.

Appendix A. Supplementary data

Supplementary data to this article can be found online at https://doi.org/10.1016/j.chemgeo.2023.121346.

References

- Agterhuis, T., Ziegler, M., de Winter, N.J., Lourens, L.J., 2022. Warm deep-sea temperatures across Eocene thermal Maximum 2 from clumped isotope thermometry. Commun. Earth. Environ. 3, 1–9.
- Allen, J.A., 1958. On the basic form and adaptations to habitat in the Lucinacea (Eulamellibranchia). Royal Soc. London 241, 421–484.
- Anderson, N.T., Kelson, J.R., Kele, S., Daëron, M., Bonifacie, M., Horita, J., Mackey, T.J., John, C.M., Kluge, T., Petschnig, P., Jost, A.B., Huntington, K.W., Bernasconi, S.M., Bergmann, K.D., 2021. A unified clumped isotope thermometer calibration (0.5–1,100°C) using carbonate-based standardization. Geophys. Res. Lett. 48.
- Bernasconi, S.M., Daëron, M., Bergmann, K.D., Bonifacie, M., Meckler, A.N., Affek, H.P., Anderson, N., Bajnai, D., Barkan, E., Beverly, E., Blamart, D., Burgener, L., Calmels, D., Chaduteau, C., Clog, M., Davidheiser-Kroll, B., Davies, A., Dux, F., Eiler, J., Elliott, B., Fetrow, A.C., Fiebig, J., Goldberg, S., Hermoso, M., Huntington, K.W., Hyland, E., Ingalls, M., Jaggi, M., John, C.M., Jost, A.B., Katz, S., Kelson, J., Kluge, T., Kocken, I.J., Laskar, A., Leutert, T.J., Liang, D., Lucarelli, J., Mackey, T.J., Mangenot, X., Meinicke, N., Modestou, S.E., Müller, I.A., Murray, S., Neary, A., Packard, N., Passey, B.H., Pelletier, E., Petersen, S., Piasecki, A., Schauer, A., Snell, K.E., Swart, P.K., Tripati, A., Upadhyay, D., Vennemann, T., Winkelstern, I., Yarian, D., Yoshida, N., Zhang, N., Ziegler, M., 2021. InterCarb: A community effort to improve interlaboratory standardization of the carbonate clumped isotope thermometer using carbonate standards. Geochem. Geophys. Geosyst. 22.
- Bigatti, G., Peharda, M., Taylor, J.D., 2004. Size at first maturity, oocyte envelopes and external morphology of sperm in three species of lucinidae (Mollusca: Bivalvia) from Coastal nursery habitats: patterns and processes of demographic variability in marine fish species along the eastern Adriatic coast View project Sclerochronology as a tool for detecting long-term Adriatic environmental changes-SCOOL View project. Malacologia 46, 417–426.
- Brissac, T., Merçot, H., Gros, O., 2011. Lucinidae/sulfur-oxidizing bacteria: Ancestral heritage or opportunistic association? Further insights from the Bohol Sea (the Philippines). FEMS Microbiol. Ecol. 75, 63–76.
- Caldarescu, D.E., Sadatzki, H., Andersson, C., Schäfer, P., Fortunato, H., Meckler, A.N., 2021. Clumped isotope thermometry in bivalve shells: A tool for reconstructing seasonal upwelling. Geochim. Cosmochim. Acta 294, 174–191.
- Corrège, T., 2006. Sea surface temperature and salinity reconstruction from coral geochemical tracers. Palaeogeogr. Palaeoclimatol. Palaeoecol. 232, 408–428.
- Culotta, E., 1988. Predators and Available Prey: Naricid Predation during a Neocene Molluscan Extinction Event.
- Daëron, M., Blamart, D., Peral, M., Affek, H.P., 2016. Absolute isotopic abundance ratios and the accuracy of $\Delta47$ measurements. Chem. Geol. 442, 83–96.
- Defliese, W.F., Hren, M.T., Lohmann, K.C., 2015. Compositional and temperature effects of phosphoric acid fractionation on δ 47 analysis and implications for discrepant calibrations. Chem. Geol. 396, 51–60.
- Eagle, R.A., Eiler, J.M., Tripati, A.K., Ries, J.B., Freitas, P.S., Hiebenthal, C., Wanamaker, A.D., Taviani, M., Elliot, M., Marenssi, S., Nakamura, K., Ramirez, P., Roy, K., 2013. The influence of temperature and seawater carbonate saturation state on ¹³C-¹⁸O bond ordering in bivalve mollusks. Biogeosciences 10, 4591–4606.
- Eiler, J.M., 2007. "Clumped-isotope" geochemistry-the study of naturally-occurring, multiply-substituted isotopologues. Earth Planet. Sci. Lett. 262, 309–327.
- Eiler, J.M., 2011. Paleoclimate Reconstruction using Carbonate Clumped Isotope Thermometry.
- Epstein, B.S., Buchsbacm, J., Lowenstam, H.A., Ukey, H.C., 1953. Revised Carbonatewater Isotopic Temperature Scale.
- Ghosh, P., Adkins, J., Affek, H., Balta, B., Guo, W., Schauble, E.A., Schrag, D., Eiler, J.M., 2006. ¹³C-¹⁸O bonds in carbonate minerals: A new kind of paleothermometer. Geochim. Cosmochim. Acta 70, 1439–1456.
- Gillikin, D.P., Lorrain, A., Navez, J., Taylor, J.W., André, L., Keppens, E., Baeyens, W., Dehairs, F., 2005. Strong biological controls on Sr/Ca ratios in aragonitic marine bivalve shells. Geochem. Geophys. Geosyst. 6.
- Henkes, G.A., Passey, B.H., Wanamaker, A.D., Grossman, E.L., Ambrose, W.G., Carroll, M.L., 2013. Carbonate clumped isotope compositions of modern marine mollusk and brachiopod shells. Geochim. Cosmochim. Acta 106, 307–325.
- Huyghe, D., Daëron, M., de Rafelis, M., Blamart, D., Sébilo, M., Paulet, Y.M., Lartaud, F., 2022. Clumped isotopes in modern marine bivalves. Geochim. Cosmochim. Acta 316, 41–58
- Ivany, L.C., 2012. Reconstructing paleoseasonality from accretionary skeletal carbonates-challenges and opportunities. Paleontol. Soc. Pap. 18, 133–165.
- Ivany, L.C., Judd, E.J., 2021. Deciphering Temperature Seasonality in Earth's Ancient Oceans. Annu. Rev. Earth Planet. Sci. 1–30.

- Jones, D.S., Quitmyer, I.R., Andrus, C.F.T., 2005. Oxygen isotopic evidence for greater seasonality in Holocene shells of *Donax variabilis* from Florida. Palaeogeogr. Palaeoclimatol. Palaeoecol. 96–108.
- Jones, M.M., Petersen, S., v. and Curley A. N., 2022. A Tropically Hot Mid-Cretaceous North American Western Interior Seaway. Geology, pp. 1–27.
- Keating-Bitonti, C.R., Ivany, L.C., Affek, H.P., Douglas, P., Samson, S.D., 2011. Warm, not super-hot, temperatures in the early Eocene subtropics. Geology 39, 771–774.
- Kelson, J.R., Huntington, K.W., Schauer, A.J., Saenger, C., Lechler, A.R., 2017. Toward a universal carbonate clumped isotope calibration: Diverse synthesis and preparatory methods suggest a single temperature relationship. Geochim. Cosmochim. Acta 197, 104–131.
- Kim, S.T., Mucci, A., Taylor, B.E., 2007. Phosphoric acid fractionation factors for calcite and aragonite between 25 and 75 °C: Revisited. Chem. Geol. 246, 135–146.
- Leder, J.J., Swart, P.K., Szmant, A.M., Dodge, R.E., 1996. The origin of variations in the isotopic record of scleractinian coral: I. Oxygen. Geochim. Cosmochim. Acta 60, 2857–2870.
- LeGrande, A.N., Schmidt, G.A., 2006. Global gridded data set of the oxygen isotopic composition in seawater. Geophys. Res. Lett. 33.
- López-Rocha, J.A., Fernández-Rivera Melo, F.J., Gastélum-Nava, E., Larios-Castro, E., 2021. Abundance and harvest strategy of three species of clam (Bivalvia: Veneridae) located in new fishing banks in the Gulf of California. Aquac. Fish. 6, 506–512.
- Mackey, T.J., Jost, A.B., Creveling, J.R., Bergmann, K.D., 2020. A decrease to low carbonate clumped isotope temperatures in cryogenian strata. AGU Adv. 1.
- Negrón, J.F., Cain, B., 2019. Mountain pine beetle in Colorado: A story of changing forests. J. For. 117, 144–151.
- Nghiem, S.V., Hall, D.K., Mote, T.L., Tedesco, M., Albert, M.R., Keegan, K., Shuman, C.A., DiGirolamo, N.E., Neumann, G., 2012. The extreme melt across the Greenland ice sheet in 2012. Geophys. Res. Lett. 39.
- O'hora, H.E., Sierra, B., Petersen, V., Vellekoop, J., Jones, M.M., Scholz, S.R., 2022. Clumped-isotope-derived climate trends leading up to the end-cretaceous mass extinction in northwest Europe. Clim. Past 1–28.
- Petersen, S.V., Defliese, W.F., Saenger, C., Daëron, M., Huntington, K.W., John, C.M., Kelson, J.R., Bernasconi, S.M., Colman, A.S., Kluge, T., Olack, G.A., Schauer, A.J., Bajnai, D., Bonifacie, M., Breitenbach, S.F.M., Fiebig, J., Fernandez, A.B., Henkes, G. A., Hodell, D., Katz, A., Kele, S., Lohmann, K.C., Passey, B.H., Peral, M.Y., Petrizzo, D.A., Rosenheim, B.E., Tripati, A., Venturelli, R., Young, E.D., Winkelstern, I.Z., 2019. Effects of improved ¹⁷O correction on interlaboratory agreement in clumped isotope calibrations, estimates of mineral-specific offsets, and temperature dependence of acid digestion fractionation. Geochem. Geophys. Geosyst. 20, 3495–3519.
- Rosenheim, B.E., Swart, P.K., Thorrold, S.R., Willenz, P., Berry, L., Latkoczy, C., 2004. High-resolution Sr/ca records in sclerosponges calibrated to temperature in situ. Geology 32, 145–148.
- Schmid, T.W., Bernasconi, S.M., 2010. An automated method for "clumped-isotope" measurements on small carbonate samples. Rapid Commun. Mass Spectrom. 24, 1955–1963.
- Schmidt, G.A., 1999. Forward modeling of carbonate proxy data from planktonic foraminifera using oxygen isotope tracers in a global ocean model. Paleoceanography 14, 482–497.
- Schöne, B.R., Freyre Castro, A.D., Fiebig, J., Houk, S.D., Oschmann, W., Kröncke, I., 2004. Sea surface water temperatures over the period 1884-1983 reconstructed from oxygen isotope ratios of a bivalve mollusk shell (Arctica islandica, southern North Sea). Palaeogeogr. Palaeoclimatol. Palaeogeol. 212. 215–232.

- Shackleton, N.J., 1973. Oxygen isotope analysis as a means of determining season of occupation of prehistoric midden sites. Archaeometry 15, 133–141.
- Spooner, P.T., Guo, W., Robinson, L.F., Thiagarajan, N., Hendry, K.R., Rosenheim, B.E., Leng, M.J., 2016. Clumped isotope composition of cold-water corals: A role for vital effects? Geochim. Cosmochim. Acta 179, 123–141.
- Taylor, J.D., Glover, E.A., 2000. Functional anatomy, chemosymbiosis and evolution of the Lucinidae. Geol. Soc. London 177, 207–225.
- Taylor, J.D., Glover, E.A., 2006. Lucinidae (Bivalvia)-the most diverse group of chemosymbiotic molluscs. Zool. J. Linnean Soc. 148, 421–438.
- Taylor, J.D., Bigatti, G., David, Ball A., 2004. Extraordinary flexible shell sculpture: the structure and formation of calcified periostracal lamellae in Lucina pensylvanica (Bivalvia: Lucinidae) Data in Malacologia - Sclerochronology as a tool for detecting long-term Adriatic environmental changes-SCOOL View project. Malacologia 46, 277–294.
- Thiagarajan, N., Adkins, J., Eiler, J., 2011. Carbonate clumped isotope thermometry of deep-sea corals and implications for vital effects. Geochim. Cosmochim. Acta 75, 4416–4425.
- Tierney, J.E., Zhu, J., King, J., Malevich, S.B., Hakim, G.J., Poulsen, C.J., 2020. Glacial cooling and climate sensitivity revisited. Nature 584, 569–573.
- Tosic, M., Restrepo, J.D., Lonin, S., Izquierdo, A., Martins, F., 2019. Water and sediment quality in Cartagena Bay, Colombia: Seasonal variability and potential impacts of pollution. Estuar. Coast. Shelf Sci. 216, 187–203.
- Tripati, A.K., Eagle, R.A., Thiagarajan, N., Gagnon, A.C., Bauch, H., Halloran, P.R., Eiler, J.M., 2010. 13C-18O isotope signatures and "clumped isotope" thermometry in foraminifera and coccoliths. Geochim. Cosmochim. Acta 74, 5697–5717.
- Trofimova, T., Milano, S., Andersson, C., Bonitz, F.G.W., Schöne, B.R., 2018. Oxygen isotope composition of Arctica islandica aragonite in the context of shell architectural organization: implications for paleoclimate reconstructions. Geochem. Geophys. Geosyst. 19, 453–470.
- Wacker, U., Fiebig, J., Tödter, J., Schöne, B.R., Bahr, A., Friedrich, O., Tütken, T., Gischler, E., Joachimski, M.M., 2014. Empirical calibration of the clumped isotope paleothermometer using calcites of various origins. Geochim. Cosmochim. Acta 141, 127–144.
- Wanamaker, A.D., Kreutz, K.J., Schöne, B.R., Maasch, K.A., Pershing, A.J., Borns, H.W., Introne, D.S., Feindel, S., 2009. A late Holocene paleo-productivity record in the western Gulf of Maine, USA, inferred from growth histories of the long-lived ocean quahog (Arctica islandica). Int. J. Earth Sci. 98, 19–29.
- Wanamaker, A.D., Kreutz, K.J., Schöne, B.R., Introne, D.S., 2011. Gulf of Maine shells reveal changes in seawater temperature seasonality during the medieval climate Anomaly and the Little Ice Age. Palaeogeogr. Palaeoclimatol. Palaeoecol. 302, 43–51.
- de Winter, N., Agterhuis, T., Ziegler, M., 2021. Optimizing sampling strategies in highresolution paleoclimate records. Clim. Past 1–52.
- Yanes, Y., Kowalewski, M., Romanek, C.S., 2012. Seasonal variation in ecological and taphonomic processes recorded in shelly death assemblages. Palaios 27, 373–385. Zhang, J.Z., Petersen, S.V., Winkelstern, I.Z., Lohmann, K.C., 2021. Seasonally variable
- Zhang, J.Z., Petersen, S.V., Winkelstern, I.Z., Lohmann, K.C., 2021. Seasonally variable aquifer discharge and cooler climate in Bermuda during the last interglacial revealed by subannual clumped isotope analysis. Paleoceanogr. Paleoclimatol. 36, 1–19.
- Zhou, G.-T., Zheng, Y.-F., 2003. An experimental study of oxygen isotope fractionation between inorganically precipitated aragonite and water at low temperatures. Geochim. Cosmochim. Acta 67, 387–399.